A Continental-Scale Investigation of Factors Controlling the Vulnerability of Soil Organic Matter in Mineral Horizons to Decomposition

Tyler Lorenz Weiglein

Thesis submitted to the faculty of the Virginia Polytechnic Institute and State University in partial fulfillment of the requirements for the degree of

Master of Science
In
Forest Resources and Environmental Conservation

Brian D. Strahm (Chair)
J. E. Barrett
Jeff A. Hatten
R. Quinn Thomas

June 26, 2019
Blacksburg, VA

Keywords: National Ecological Observatory Network, carbon, nitrogen, incubation, two-pool model, proximal controls, non-crystalline minerals

A Continental-Scale Investigation of Factors Controlling the Vulnerability of Soil Organic Matter in Mineral Horizons to Decomposition

Tyler Lorenz Weiglein

ABSTRACT

Soil organic matter (SOM) is the largest terrestrial pool of organic carbon (C), and potential carbon-climate feedbacks involving SOM decomposition could exacerbate anthropogenic climate change. Despite the importance of SOM in the global C cycle, our understanding of the controls on SOM stabilization and decomposition is still developing, and as such, SOM dynamics are a source of major uncertainty in current Earth system models (ESMs), which reduces the effectiveness of these models in predicting the efficacy of climate change mitigation strategies. To improve our understanding of controls on SOM decomposition at scales relevant to such modeling efforts, A and upper B horizon soil samples from 22 National Ecological Observatory Network (NEON) sites spanning the conterminous U.S. were incubated for 52 weeks under conditions representing site-specific mean summer temperature and horizon-specific field capacity (-33 kPa) water potential. Cumulative CO_2 respired was periodically measured and normalized by soil organic C content to obtain cumulative specific respiration (CSR). A two-pool decomposition model was fitted to the CSR data to calculate decomposition rates of fast- (k_{fast}) and slow-cycling pools (k_{slow}). Post-LASSO best subsets multiple linear regression was used to construct horizon-specific models of significant predictors for CSR, k_{fast}, and k_{slow}. Significant predictors for all three response variables consisted mostly of proximal

factors related to clay-sized fraction mineralogy and SOM composition. Non-crystalline minerals and lower SOM lability negatively affected CSR for both A and B horizons. Significant predictors for decomposition rates varied by horizon and pool. B horizon decomposition rates were positively influenced by nitrogen (N) availability, while an index of pyrogenic C had a negative effect on k_{fast} in both horizons. These results reinforce the recognized need to explicitly represent SOM stabilization via interactions with non-crystalline minerals in ESMs, and they also suggest that increased N inputs could enhance SOM decomposition in the subsoil, highlighting another mechanism beyond shifts in temperature and precipitation regimes that could alter SOM decomposition rates.

GENERAL AUDIENCE ABSTRACT

Soils contain a large amount of carbon (C) in the form of soil organic matter (SOM), and there is the potential for the increased decomposition of SOM due to warmer temperatures to cause climate change to become worse through the release of additional CO_2 into the atmosphere. However, we still do not know exactly what is most important for predicting how vulnerable SOM is to decomposition at continental scales, and this results in a substantial amount of uncertainty in Earth system models used to predict climate change. To address this question, the proportion of organic C decomposed in soil samples from the topsoil and subsoil from 22 sites across the conterminous U.S. was monitored over the course of a year under optimal moisture conditions and at site-specific summer temperature. Additionally, a mathematical model was fitted to the proportion of organic C decomposed over time to estimate decomposition rates of a quickly decomposing pool of SOM and a slowly decomposing pool of SOM. The proportion of organic C decomposed and decomposition rates were related to soil and site properties using multiple linear regression to find which soil and site properties were most important for predicting these response variables. The type of clay-sized mineral and SOM chemical composition were found to be important predictors of the proportion of organic C decomposed for both topsoil and subsoil samples. The important predictors for decomposition rates varied by pool and by topsoil vs. subsoil. For subsoil decomposition rates, it was found that a greater availability of nitrogen (N) increased decomposition rates, and in the quickly decomposing pool, it was found that fire-derived organic matter slowed decomposition rates. The results of this study showed the general importance of local factors for controlling SOM

decomposition. Specifically, it showed that the type of clay-sized mineral present at a site needs to be considered as well as the fact that N might increase SOM decomposition in the subsoil.

DEDICATION

I would like to dedicate this work to my maternal grandfather, Donald Kerr, for encouraging my curiosity as a child by letting me take apart far more things than I could put back together and to my mother, Janice Weiglein, for encouraging my interest in Earth science from an early age.

ACKNOWLEDGEMENTS

This project was funded by the U.S. National Science Foundation under awards EF-1340681 and DBI-1724433. I would like to acknowledge the National Ecological Observatory Network Systems Installation and Verification Team for their work in collecting the soil cores used in this study. I would also like to acknowledge the entire SOMMOS team, Mike SanClements, Adrian Gallo, Jeff Hatten, Kate Heckman, and Luke Nave, without whom this project would not be possible, and I would like to give a special acknowledgement to Adrian for all his work in describing and processing 200 some soil cores at Oregon State University. Also, I would like to thank Brian Strahm, my advisor and also a member of the SOMMOS team, for his insightful feedback throughout the course of this project. Additionally, I would like to thank Stephanie Duston and Dave Mitchem for their assistance with laboratory work here at Virginia Tech. Lastly, I would like to thank my family for their love and support and my FREC graduate student cohort for the many fond memories.

TABLE OF CONTENTS

LIST OF FIGURES

LIST OF TABLES

ATTRIBUTION

In accordance with the requirements of the Virginia Tech Graduate School for theses following the manuscript format, this section specifies the contribution of listed co-authors in the included manuscript (Ch. 2). As of the submission of this thesis, the manuscript was written solely by Tyler Weiglein with feedback from Brian Strahm. Feedback from the other co-authors will be sought prior to submission of the manuscript for publication.

CH. 1: INTRODUCTION AND BACKGROUND INFORMATION

Introduction

Soil organic matter (SOM) is the largest actively cycled terrestrial pool of organic carbon (C) and is directly linked to climate through SOM decomposition and subsequent CO_2 evolution. Recent estimates of SOM C stocks in the upper 1 m of soil range from 1325 Pg C to 1502 Pg C (Jobbagy & Jackson, 2000; Köchy, Hiederer, & Freibauer, 2015), while SOM C stocks to a depth of 3 m or greater range from 2344 Pg C to approximately 3000 Pg C (Jobbagy & Jackson, 2000; Köchy et al., 2015; Tarnocai et al., 2009). In contrast, the terrestrial vegetation C pool has been estimated to be between 466 Pg C and 654 Pg C (Prentice et al., 2001). Likewise, the atmospheric C pool in 2017 was estimated to be 860 Pg C (Le Quéré et al., 2018). Given the size of the SOM C pool relative to other actively cycled C pools and the linkages between SOM decomposition and climate, there is the potential for carbon-climate feedbacks that could exacerbate climate change due to anthropogenic radiative forcing (e.g., increased atmospheric greenhouse gas concentrations, changes in surface albedo).

The evidence for a carbon-climate feedback involving SOM decomposition is inconclusive. Data show that soil respiration, which consists of both belowground autotrophic respiration (e.g., root respiration) and heterotrophic respiration (e.g., SOM decomposition), has increased on a global scale due to increased temperatures (Bond-Lamberty & Thomson, 2010). Furthermore, a recent analysis has demonstrated that the ratio of heterotrophic soil respiration (SOM decomposition) to total soil respiration has increased globally between 1990 and 2014 (Bond-Lamberty, Bailey, Chen, Gough, & Vargas, 2018). However, it remains unclear whether

this increase in respiration is due to the decomposition of older, stabilized SOM or newer, labile C inputs from plants. Bellamy, Loveland, Bradley, Lark, & Kirk (2005) report widespread C losses in highly organic soils in England and Wales over the past several decades due to warming; in contrast, Hopkins *et al.* (2009) found no significant change in SOM C stocks in permanent grasslands in England over a similar period of time. Consequently, we still do not have a thorough understanding of how SOM C stocks will respond to global change drivers, and this knowledge gap, which is attributed in part to an ongoing paradigm shift in regards to SOM stabilization (Todd-Brown et al., 2013), is a major source of uncertainty in current Earth system models (Friedlingstein et al., 2014), which affects society's ability to accurately predict the efficacy of various climate change mitigation strategies.

SOM Stabilization Paradigm Shift

SOM consists of a complex mixture of plant residues, microbial products, and pyrogenic (fire-derived) material. Historically, it was believed that stable SOM, that is SOM that remains in the soil for an extended period of time (e.g., decades to millennia), was formed through either the selective preservation of chemically recalcitrant plant residues or the formation of amorphous, chemically complex humic substances that were inherently resistant to decomposition (Lehmann & Kleber, 2015; Schmidt et al., 2011). However, the paradigm that has emerged over the past decade places less emphasis on the chemical properties of SOM (at least in mineral soils) and instead posits that soil physicochemical properties (e.g., pH, mineralogy of the clay-sized fraction) and other ecosystem properties (e.g., vegetation, climate) are the dominant factors controlling SOM stabilization (Lehmann & Kleber, 2015; Schmidt et al., 2011). Additionally, the

importance of microbial communities in the formation of stable SOM has been recognized in recently proposed conceptual models (Cotrufo, Wallenstein, Boot, Denef, & Paul, 2013; Liang, Schimel, & Jastrow, 2017) with direct evidence of their contribution to the formation of SOM recently provided (Kallenbach, Frey, & Grandy, 2016).

With this paradigm shift, a new suite of stabilization mechanisms (in addition to the chemical composition of SOM) has been identified (Fig. 1.1) including (i) occlusion within aggregates, (ii) mineral-organic matter interactions, (iii) formation of pyrogenic C (which could be considered a part of the SOM chemical composition stabilization mechanism), (iv) climatic factors (e.g., xeric conditions, extreme temperatures), and (v) local environmental conditions (e.g., low O_2 levels) (Schmidt et al., 2011; Sollins, Homann, & Caldwell, 1996; von Lützow et al., 2006).

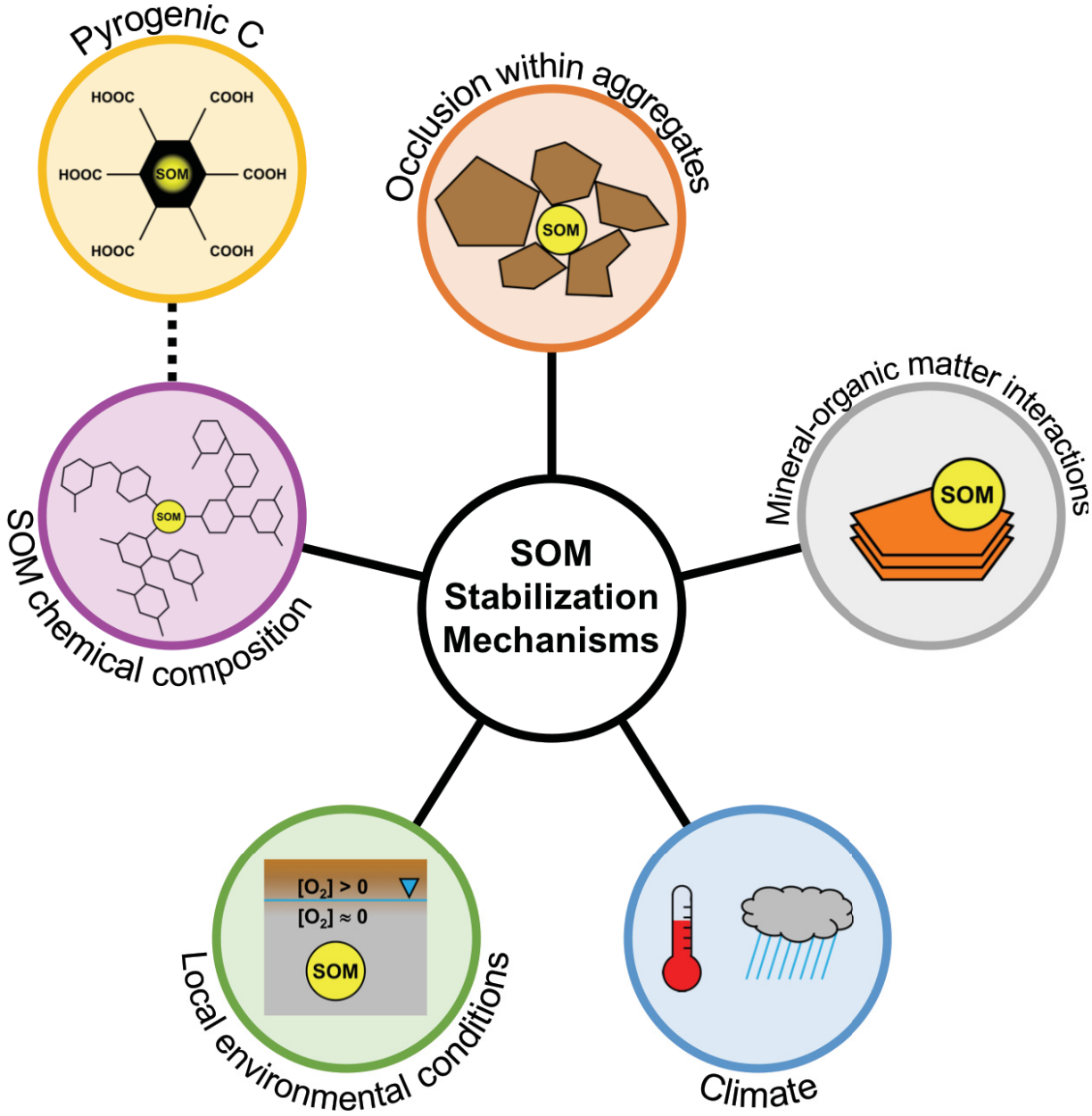

Figure 1.1 Suite of SOM stabilization mechanisms consistent with the contemporary SOM stabilization paradigm.

Need for Suite of Continental-Scale Predictors of SOM Vulnerability

The modeling community has come to recognize the need for more explicit representation of SOM stabilization mechanisms in Earth system models (ESMs) (Todd-Brown et al., 2013). However, if studies of SOM dynamics are to be of use to Earth system modelers, the studies must move beyond single sites (Trumbore, 2009). Instead, they must follow in the footsteps of previous studies related to SOM cycling that have demonstrated broad-scale relationships (e.g., Burke et al., 1989; Lloyd & Taylor, 1994; Post, Emanuel, Zinke, & Stangenberger, 1982). Consequently, these studies must leverage large-scale (i.e., continental-scale) sample sets, such as that provided by the National Ecological Observatory Network (NEON). Additionally, because of the failure to find a simple predictor for the vulnerability of SOM to global change (Dungait, Hopkins, Gregory, & Whitmore, 2012), these studies must consider the effect of multiple SOM stabilization mechanisms that result in more nuanced large-scale relationships (von Lützow & Kögel-Knabner, 2009).

Furthermore, studies focusing on the vulnerability of SOM must define what, specifically, is meant by vulnerability. For this study, the definition of vulnerability is cumulative specific respiration (CSR), or the proportion of soil organic C respired (e.g., $\mu g\ CO_2\text{-}C\ (g\ C)^{-1}$), over the course of a 52-week laboratory incubation. Although laboratory incubations can have several limitations, including artificial temperature and moisture regimes, destruction of soil structure, and the exclusion of plant inputs, they do allow for the evaluation of SOM decomposition dynamics under controlled experimental conditions (Torn, Swanston, Castanha, & Trumbore, 2009), more easily allowing for cross-site comparisons. To better understand the decomposition dynamics in our samples, a two-pool decomposition model was fitted to our CSR

data to provide estimates of the decomposition rates for a fast-cycling pool and a slow-cycling pool.

Objectives

The purpose of this study was to leverage a broadly distributed soil sample set from NEON spanning a wide range of climates, vegetation covers, land uses, and soil types to address the question of what factors predict the vulnerability of SOM to decomposition at a large (i.e., continental) scale. Specifically, the study had two objectives, which are listed below.

Objective 1: Predictors of cumulative specific respiration

The project's first objective was to determine (i) which factors are significant predictors of cumulative specific respiration and (ii) whether these factors differed by horizon (i.e., A vs. upper B).

Objective 2: Predictors of decomposition rates

The project's second objective was to determine (i) which factors are significant predictors of two-pool model decomposition rates, (ii) whether these factors differed by pool (i.e., fast vs. slow), and (iii) whether these factors differed by horizon (i.e., A vs. upper B).

Hypotheses

Objective 1: Predictors of cumulative specific respiration

It was predicted that proxies of the stabilization mechanisms shown in Figure 1.1 (excluding occlusion within aggregates due to the sieving of the soil samples) would be negatively correlated with cumulative specific respiration. Additionally, it was predicted that the magnitude of the effect of different stabilization mechanisms would vary with horizon (Sollins et al., 1996; M. von Lützow et al., 2006). Given our emerging understanding of the importance of non-crystalline minerals in controlling SOM dynamics (e.g., Doetterl et al., 2015; Rasmussen et al., 2018; Torn, Trumbore, Chadwick, Vitousek, & Hendricks, 1997), it was predicted that non-crystalline minerals in particular would play a dominant role in controlling cumulative specific respiration.

Objective 2: Predictors of decomposition rates

As above, it was predicted that proxies of at least some of the stabilization mechanisms shown in Figure 1.1 would be significant predictors of fitted decomposition rates. Specifically, given previous work demonstrating the dominant role played by chemical composition in controlling decomposition rates (e.g., Melillo, Aber, & Muratore, 1982), it was predicted that SOM chemical composition would be an important predictor of decomposition rates. Additionally, it was predicted that significant predictors would vary by pool and by horizon.

References

Bellamy, P. H., Loveland, P. J., Bradley, R. I., Lark, R. M., & Kirk, G. J. D. (2005). Carbon losses from all soils across England and Wales 1978–2003. *Nature*, *437*(7056), 245–248.

Bond-Lamberty, B., Bailey, V. L., Chen, M., Gough, C. M., & Vargas, R. (2018). Globally rising soil heterotrophic respiration over recent decades. *Nature*, *560*(7716), 80–83.

Bond-Lamberty, B., & Thomson, A. (2010). Temperature-associated increases in the global soil respiration record. *Nature*, *464*(7288), 579–582.

Burke, I. C., Yonker, C. M., Parton, W. J., Cole, C. V., Schimel, D. S., & Flach, K. (1989). Texture, Climate, and Cultivation Effects on Soil Organic Matter Content in U.S. Grassland Soils. *Soil Science Society of America Journal*, *53*(3), 800.

Cotrufo, M. F., Wallenstein, M. D., Boot, C. M., Denef, K., & Paul, E. (2013). The Microbial Efficiency-Matrix Stabilization (MEMS) framework integrates plant litter decomposition with soil organic matter stabilization: Do labile plant inputs form stable soil organic matter? *Global Change Biology*, *19*(4), 988–995.

Doetterl, S., Stevens, A., Six, J., Merckx, R., Van Oost, K., Casanova Pinto, M., … Boeckx, P. (2015). Soil carbon storage controlled by interactions between geochemistry and climate. *Nature Geoscience*, *8*(10), 780–783.

Dungait, J. A. J., Hopkins, D. W., Gregory, A. S., & Whitmore, A. P. (2012). Soil organic matter turnover is governed by accessibility not recalcitrance. *Global Change Biology*, *18*(6), 1781–1796.

Friedlingstein, P., Meinshausen, M., Arora, V. K., Jones, C. D., Anav, A., Liddicoat, S. K., … Knutti, R. (2014). Uncertainties in CMIP5 Climate Projections due to Carbon Cycle

Feedbacks. *Journal of Climate*, *27*(2), 511–526.

Hopkins, D. W., Waite, I. S., McNicol, J. W., Poulton, P. R., Macdonald, A. J., & O'Donnell, A. G. (2009). Soil organic carbon contents in long-term experimental grassland plots in the UK (Palace Leas and Park Grass) have not changed consistently in recent decades. *Global Change Biology*, *15*(7), 1739–1754.

Jobbagy, E. G., & Jackson, R. B. (2000). The vertical distribution of soil organic carbon and its relation to climate and vegetation. *Ecological Applications*, *10*(2), 423–436.

Kallenbach, C. M., Frey, S. D., & Grandy, A. S. (2016). Direct evidence for microbial-derived soil organic matter formation and its ecophysiological controls. *Nature Communications*, *7*, 13630.

Köchy, M., Hiederer, R., & Freibauer, A. (2015). Global distribution of soil organic carbon – Part 1: Masses and frequency distributions of SOC stocks for the tropics, permafrost regions, wetlands, and the world. *SOIL*, *1*(1), 351–365.

Le Quéré, C., Andrew, R., Friedlingstein, P., Sitch, S., Hauck, J., Pongratz, J., … Zheng, B. (2018). Global Carbon Budget 2018. *Earth System Science Data*, *10*(4), 2141–2194.

Lehmann, J., & Kleber, M. (2015). The contentious nature of soil organic matter. *Nature*, *528*, 60–68.

Liang, C., Schimel, J. P., & Jastrow, J. D. (2017). The importance of anabolism in microbial control over soil carbon storage. *Nature Microbiology*, *2*(8), 17105.

Lloyd, J., & Taylor, J. A. (1994). On the Temperature Dependence of Soil Respiration. *Functional Ecology*, *8*(3), 315.

Melillo, J. M., Aber, J. D., & Muratore, J. F. (1982). Nitrogen and Lignin Control of Hardwood Leaf Litter Decomposition Dynamics. *Ecology*, *63*(3), 621–626.

Post, W. M., Emanuel, W. R., Zinke, P. J., & Stangenberger, A. G. (1982). Soil carbon pools and world life zones. *Nature*, *298*(5870), 156–159.

Prentice, I. C., Fasham, M. J. R., Goulden, M., Heimann, M., Jaramillo, V., Kheshgi, H., … Farquhar, G. (2001). The carbon cycle and atmospheric carbon dioxide. In J. T. Houghton, Y. Ding, D. J. Griggs, M. Noguer, P. J. van der Linden, X. Dai, & K. M. an (Eds.), *Climate Change 2001: The Scientific Basis* (pp. 183–237). Cambridge, UK: Cambridge University Press.

Rasmussen, C., Heckman, K., Wieder, W. R., Keiluweit, M., Lawrence, C. R., Berhe, A. A., … Wagai, R. (2018). Beyond clay: towards an improved set of variables for predicting soil organic matter content. *Biogeochemistry*, *137*(3), 297–306.

Schmidt, M. W. I., Torn, M. S., Abiven, S., Dittmar, T., Guggenberger, G., Janssens, I. A., … Trumbore, S. E. (2011). Persistence of soil organic matter as an ecosystem property. *Nature*, *478*(7367), 49–56.

Sollins, P., Homann, P., & Caldwell, B. A. (1996). Stabilization and destabilization of soil organic matter: Mechanisms and controls. *Geoderma*, *74*(1–2), 65–105.

Tarnocai, C., Canadell, J. G., Schuur, E. A. G., Kuhry, P., Mazhitova, G., & Zimov, S. (2009). Soil organic carbon pools in the northern circumpolar permafrost region. *Global Biogeochemical Cycles*, *23*(2), 1–11.

Todd-Brown, K. E. O., Randerson, J. T., Post, W. M., Hoffman, F. M., Tarnocai, C., Schuur, E. A. G., & Allison, S. D. (2013). Causes of variation in soil carbon simulations from CMIP5 Earth system models and comparison with observations. *Biogeosciences*, *10*(3), 1717–1736.

Torn, M. S., Swanston, C. W., Castanha, C., & Trumbore, S. E. (2009). Storage and Turnover of Organic Matter in Soil. In *Biophysico-Chemical Processes Involving Natural Nonliving*

Organic Matter in Environmental Systems (pp. 219–272).

Torn, M. S., Trumbore, S. E., Chadwick, O. A., Vitousek, P. M., & Hendricks, D. M. (1997). Mineral control of soil organic carbon storage and turnover. *Nature*, *389*(6647), 170–173.

Trumbore, S. (2009). Radiocarbon and Soil Carbon Dynamics. *Annual Review of Earth and Planetary Sciences*, *37*(1), 47–66.

von Lützow, M., Kögel-Knabner, I., Ekschmitt, K., Matzner, E., Guggenberger, G., Marschner, B., & Flessa, H. (2006). Stabilization of organic matter in temperate soils: Mechanisms and their relevance under different soil conditions - A review. *European Journal of Soil Science*, *57*(4), 426–445.

von Lützow, Margit, & Kögel-Knabner, I. (2009). Temperature sensitivity of soil organic matter decomposition-what do we know? *Biology and Fertility of Soils*, *46*(1), 1–15.

CH. 2: INCUBATION RESULTS – PROXIMAL CONTROLS DOMINATE SOIL ORGANIC MATTER DECOMPOSITION POTENTIAL IN MINERAL SOILS AT A CONTINENTAL SCALE

Proximal controls dominate soil organic matter decomposition potential in mineral soils at a continental scale

Dominant local controls on SOM decomposition (running title)

Tyler Weiglein[1], Brian Strahm[1], Michael SanClements[2,3], Adrian Gallo[4], Jeff Hatten[5], Katherine Heckman[6], and Lucas Nave[7]

[1]Department of Forest Resources and Environmental Conservation, Virginia Tech, Blacksburg, VA, USA

[2]National Ecological Observatory Network, Boulder, CO, USA

[3]Institute of Arctic and Alpine Research, University of Colorado Boulder, Boulder, CO, USA

[4] Crop and Soil Science, Oregon State University, Corvallis, OR, USA

[5]Forest Engineering, Resources and Management, Oregon State University, Corvallis, OR, USA

[6]Northern Institute of Applied Climate Science, USDA Forest Service, Houghton, MI, USA

[7]University of Michigan Biological Station, Pellston, MI, USA

Correspondence: Tyler Weiglein, tel. +1 540 728 0606, e-mail: weiglein@vt.edu

Abstract

Soil organic matter (SOM) is the largest terrestrial pool of organic carbon (C), and potential carbon-climate feedbacks involving SOM decomposition could exacerbate anthropogenic climate change. Despite the importance of SOM in the global C cycle, our understanding of the controls on SOM stabilization and decomposition is still developing, and as such, SOM dynamics are a source of major uncertainty in current Earth system models (ESMs). To improve our understanding of controls on SOM decomposition at scales relevant to such modeling efforts, A and upper B horizon soil samples from 22 National Ecological Observatory Network (NEON) sites spanning the conterminous U.S. were incubated for 52 weeks under conditions representing site-specific mean summer temperature and horizon-specific field capacity (-33 kPa) water potential. Cumulative CO_2 respired was periodically measured and normalized by soil organic C content to obtain cumulative specific respiration (CSR). A two-pool decomposition model was fitted to the CSR data to calculate decomposition rates of fast- (k_{fast}) and slow-cycling pools (k_{slow}). Post-LASSO best subsets multiple linear regression was used to construct horizon-specific models of significant predictors for CSR, k_{fast}, and k_{slow}. Significant predictors for all three response variables consisted mostly of proximal factors related to clay-sized fraction mineralogy and SOM composition. Non-crystalline minerals and lower SOM lability negatively affected CSR for both A and B horizons. Significant predictors for decomposition rates varied by horizon and pool. B horizon decomposition rates were positively influenced by nitrogen (N) availability, while an index of pyrogenic C had a negative effect on k_{fast} in both horizons. These results reinforce the recognized need to explicitly represent SOM stabilization via interactions with non-crystalline minerals in ESMs, and they also suggest that increased N inputs could

enhance SOM decomposition in the subsoil, highlighting another mechanism beyond shifts in temperature and precipitation regimes that could alter SOM decomposition rates.

Keywords: National Ecological Observatory Network, carbon, nitrogen, incubation, two-pool model, proximal controls, non-crystalline minerals

Introduction

Soil organic matter (SOM) is the largest actively cycled terrestrial pool of organic carbon (C) and is directly linked to climate through SOM decomposition and subsequent CO_2 evolution. Several estimates of SOM C stocks in the upper 1 m of soil range from 1325 Pg C to 1502 Pg C (Jobbagy & Jackson, 2000; Köchy et al., 2015), while estimates of SOM C stocks to a depth of 3 m or greater range from 2344 Pg C to approximately 3000 Pg C (Jobbagy & Jackson, 2000; Köchy et al., 2015; Tarnocai et al., 2009). In contrast, the terrestrial vegetation C pool has been estimated to be between 466 Pg C and 654 Pg C (Prentice et al., 2001). Likewise, the atmospheric C pool in 2017 was estimated to be 860 Pg C (Le Quéré et al., 2018). Given the size of the SOM C pool relative to other actively cycled C pools and the linkages between SOM decomposition and climate, there is the potential for an amplifying feedback between SOM decomposition and climate warming. Despite the critical role played by SOM in the global C cycle, we still do not have a thorough understanding of how SOM will respond to global change drivers. This knowledge gap, which is attributed in part to an ongoing paradigm shift in our understanding of SOM stabilization (Todd-Brown et al., 2013), is a major source of uncertainty

in current Earth system models (ESMs) (Friedlingstein et al., 2014), which affects society's ability to accurately predict the efficacy of various climate change mitigation strategies.

SOM consists of a complex mixture of plant residues and microbial products in varying states of degradation (e.g., pyrogenic material). Historically, it was believed that stable SOM, that is SOM that remains in the soil for an extended period of time (e.g., decades to millennia), was formed through either the selective preservation of chemically recalcitrant plant residues or the formation of amorphous, chemically complex humic substances that are inherently resistant to decomposition (Lehmann & Kleber, 2015; Schmidt et al., 2011). However, the paradigm that has emerged over the past decade places less emphasis on the chemical properties of SOM in mineral soils and instead posits that soil physicochemical properties (e.g., pH, clay-sized fraction mineralogy) and other ecosystem properties (e.g., vegetation, climate) are the dominant factors controlling SOM stabilization (Lehmann & Kleber, 2015; Schmidt et al., 2011). With this paradigm shift, a new suite of stabilization mechanisms beyond chemical recalcitrance has been identified including: (i) occlusion within aggregates, (ii) mineral-organic matter interactions, (iii) formation of pyrogenic C (which could potentially be considered a subset of the chemical recalcitrance stabilization mechanism), (iv) climatic factors (e.g., xeric conditions, extreme temperatures), and (v) local environmental conditions (e.g., low O_2 levels) (Friedlingstein et al., 2006; Schmidt et al., 2011; Sollins, Homann, & Caldwell, 1996).

Several methods have been used to study SOM decomposition dynamics in soil, including laboratory incubations, *in situ* measurements of soil respiration, ^{13}C stable isotope studies, and radiocarbon (^{14}C) measurements (Torn, Swanston, Castanha, & Trumbore, 2009). Each method measures a slightly different aspect of SOM dynamics and has its own advantages and disadvantages. Laboratory incubations have been used to estimate a number of SOM

properties, including mean residence times (Paul, Morris, Conant, & Plante, 2006; Torn, Vitousek, & Trumbore, 2005) and stability (Swanston, Caldwell, Homann, Ganio, & Sollins, 2002; Whalen, Bottomley, & Myrold, 2000). In addition to incubations being relatively simple and allowing for controlled experimental conditions (Torn et al., 2009), the results of incubations more readily correspond to SOM properties than other artificial fractionation schemes (Paul, Collins, & Leavitt, 2001), which allow for them to be more easily used for comparative studies. However, incubations have a number of shortcomings, including artificial temperature and moisture regimes, destruction of soil structure, and the exclusion of plant inputs (Torn et al., 2009).

To accurately predict potential carbon-climate feedbacks involving SOM and to manage SOM stocks to contribute to climate change mitigation efforts, the modeling community has come to recognize the need for more explicit representation of SOM stabilization mechanisms in ESMs (Todd-Brown et al., 2013). If studies of SOM dynamics are to be of use to the development of ESMs though, these studies must move beyond single sites (Trumbore, 2009). Instead, they must follow the example of previous studies related to SOM cycling that have demonstrated broad-scale relationships (e.g., Burke et al., 1989; Lloyd & Taylor, 1994; Post et al., 1982). However, given the understanding that a number of mechanisms operate simultaneously to stabilize SOM, it remains uncertain whether relatively simple, large-scale relationships exist related to SOM stabilization (Dungait et al., 2012).

This study uses a continental-scale soil sample set from the U.S. National Science Foundation National Ecological Observatory Network (NEON) in a 52-week laboratory incubation experiment to address the question whether there are predictors that emerge at a

continental-scale that can predict SOM vulnerability to decomposition and model decomposition rates.

Materials and Methods

Sampling sites

Soil samples were taken from 22 NEON sites spanning the conterminous United States (Fig. 2.1 and Table 2.1). At each site, 10 4.5-cm soil cores were taken (2 cores from each of the 5 soil plots in the vicinity of the site's micrometeorological tower) via Giddings probe (Giddings Machine Company, Windsor, CO) up to a depth of 2 m depending on depth to bedrock. These cores were cooled with ice packs and shipped to Oregon State University for processing.

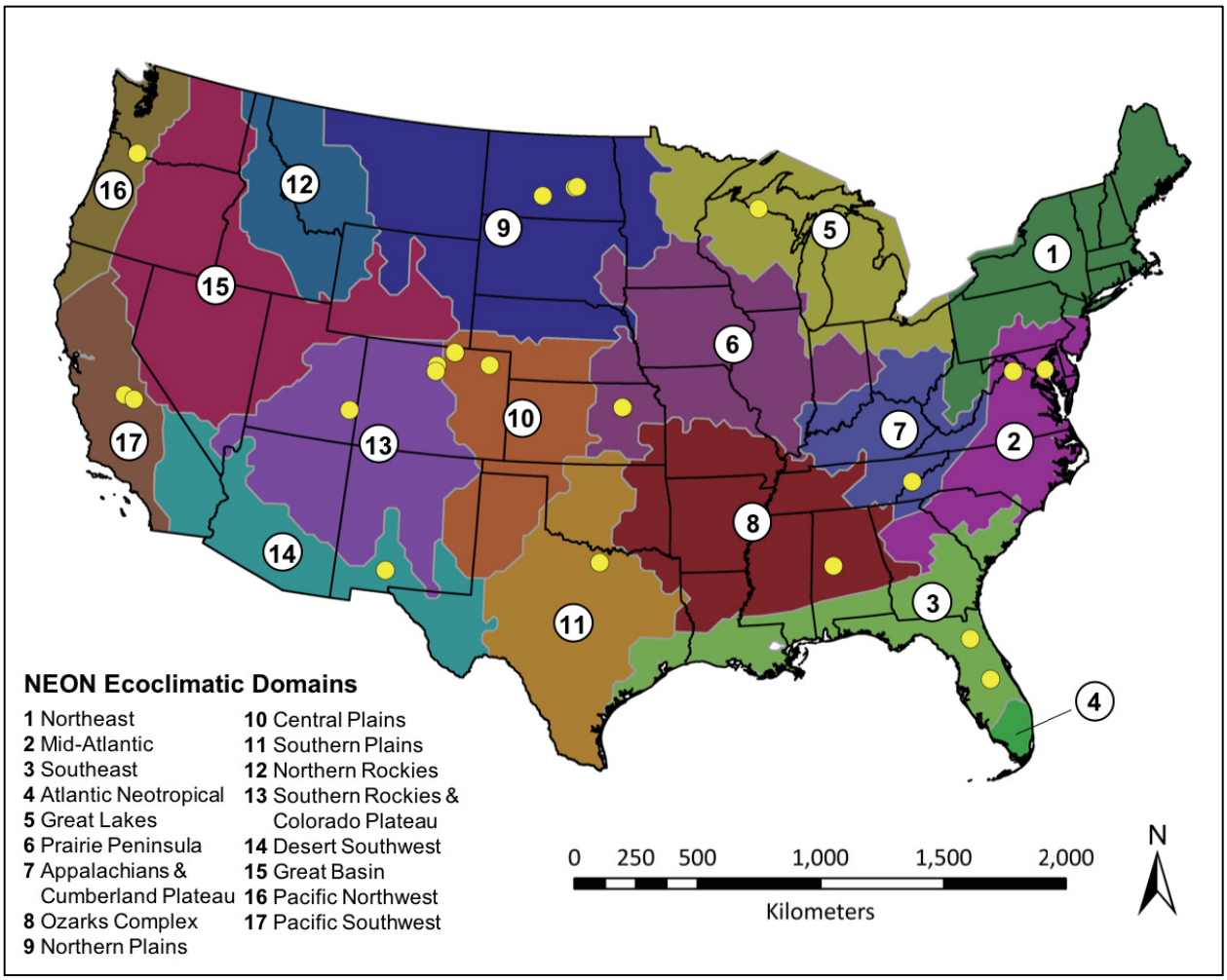

Fig. 2.1 Location of 22 National Ecological Observatory Network (NEON) sites from which soil samples were taken. The different colored zones and numbers correspond to NEON's ecoclimatic domains as specified in the legend. Note that the sites KONA and KONZ (Table 2.1) are represented by one yellow circle due to their close proximity.

Table 2.1 Site-specific location, soil order, and climate data for samples from NEON sites.

Site ID	Site Name	Latitude	Longitude	Dominant Soil Order	MAT (ºC)	MAP (mm)	MAP - PET (mm)	Incubation Temp. (ºC)
ABBY	Abby Road	45.76243	-122.33033	Andisol	10.0	2530	1845	17.5
BLAN	Blandy Experimental Farm	39.06026	-78.07164	Alfisol	12.1	950	196	22.5
CLBJ	LBJ National Grassland	33.40123	-97.57000	Alfisol	17.5	840	-559	27.5
CPER	Central Plains Experimental Range	40.81553	-104.74560	Mollisol	8.6	370	-681	20.0
DCFS	Dakota Coteau Field School	47.16165	-99.10656	Mollisol	4.9	490	-257	20.0
DSNY	Disney Wilderness Preserve	28.12504	-81.43620	Spodosol	22.5	1150	-134	27.5
GRSM	Great Smoky Mountains National Park, Twin Creeks	35.68896	-83.50195	Inceptisol	12.6	1396	569	22.5
JORN	Jornada LTER	32.59068	-106.84254	Aridisol	15.7	173	-1382	25.0
KONA	Konza Prairie Biological Station - Relocatable (Agriculture)	39.11044	-96.61295	Mollisol	12.8	860	-188	25.0
KONZ	Konza Prairie Biological Station - Core	39.10077	-96.56309	Mollisol	12.4	860	-157	25.0
MOAB	Moab	38.24833	-109.38827	Aridisol	10.2	200	-955	22.5
NGPR	Northern Great Plains Research Laboratory	46.76972	-100.91535	Mollisol	5.9	400	-400	20.0
NIWO	Niwot Ridge Mountain Research Station	40.05425	-105.58237	Inceptisol	-0.6	758	190	10.0
OSBS	Ordway-Swisher Biological Station	29.68927	-81.99343	Entisol	20.8	1290	119	27.5
RMNP	Rocky Mountain National Park, CASTNET	40.27591	-105.54592	Inceptisol	3.9	520	-306	15.0
SERC	Smithsonian Environmental Research Center	38.89008	-76.56001	Alfisol	13.5	1107	292	25.0
SJER	San Joaquin Experimental Range	37.10878	-119.73228	Alfisol	16.6	270	-1182	25.0
SOAP	Soaproot Saddle	37.03337	-119.26219	Alfisol	13.7	1246	-107	22.5
STER	North Sterling, CO	40.46190	-103.02930	Mollisol	9.7	370	-724	22.5
TALL	Talladega National Forest	32.95046	-87.39327	Ultisol	17.2	1350	378	25.0
UNDE	UNDERC	46.23388	-89.53725	Spodosol	4.3	854	205	17.5
WOOD	Woodworth	47.12823	-99.24136	Mollisol	4.9	490	-276	20.0

MAT, mean annual temperature; MAP, mean annual precipitation

Sample processing

Of the 10 cores collected per site, 5 were frozen and archived for future use, while the remaining 5 were refrigerated at 3 ºC until processing, typically within 2 weeks of arrival. After cores' liners were opened longitudinally, the cores were described according to USDA's *Soil Taxonomy* and then split by genetic horizon. Splits were composited by horizon, air-dried, and passed through a 2-mm sieve to remove rock fragments and any coarse particulate matter. Subsamples of A and upper B horizons (henceforth simply referred to as B horizons) were then sent to Virginia Tech for a 52-week laboratory incubation.

Laboratory incubation

For the laboratory incubation, 20 g of soil were placed in 118-mL polypropylene specimen cups. Samples were tamped down as needed to bulk densities representative of bulk densities in the field (1.0 g cm^{-3} for A horizons and 1.2 g cm^{-3} for B horizons). These samples were then placed into 946-mL mason jars with lids fitted with septa. A small amount of water was added to the bottom of the jars to maintain humidity in the jar headspace and minimize water loss via evaporation from the sample. Samples were brought up to field capacity (-33 kPa) by adding an amount of DI water estimated using pedotransfer functions developed by Saxton *et al.* (1986) and site-specific soil texture data. Soil texture data were obtained for all sites from NEON megapit data (NEON, 2019a) with the exception of SJER and SOAP, for which soil texture data were obtained from USDA NRCS Soil Web Survey (Soil Survey Staff, 2017).

Sites were binned by mean summer temperature, and samples were placed in their respective 566-L incubator (VWR Model 10753-894; VWR International, LLC, Radnor, PA, USA) set at a corresponding group mean summer temperature (Table 2.1). Over the course of the

52-week incubation, jar headspace samples were taken periodically (typically at least every 28 days and often more frequently to avoid exceeding headspace CO_2 concentrations of 10,000 ppm) using a syringe and injected into evacuated 10-mL gas chromatograph (GC) vials. After sampling, jars were opened to allow their headspaces to re-equilibrate with the atmosphere, and any water lost from the samples via evaporation was replenished by adding DI water. Prior to resealing the jars and placing them back in their respective incubator, an initial headspace sample was taken.

Headspace samples were analyzed for CO_2 concentrations using a GC outfitted with a methanizer and flame ionization detector (FID) (GC-2010; Shimadzu Scientific Instruments, Columbia, MD, USA).

Response variables: Cumulative specific respiration and decomposition rates

Mass of CO_2-C respired (μg CO_2-C) was calculated using the ideal gas law as shown in Eqn (1):

$$CO_2\text{-}C\ respired = \frac{\Delta[CO_2]M_C P V_{jar}}{RT} \quad (1)$$

where $\Delta[CO_2]$ is the change in CO_2 concentration (ppm), M_C is the molar mass of C (12.01 g mol^{-1}), P is pressure (assumed to be 1 atm), V_{jar} is the volume of the jar (L), R is the universal gas constant (0.08206 L atm $(mol\ K)^{-1}$), and T is the incubation temperature (K). For samples containing carbonates (as indicated by a "k" horizon suffix), an isotope mixing model was used to partition CO_2 produced from heterotrophic respiration from CO_2 produced by the dissolution of carbonates with end members determined using gas and solid phase ^{13}C measurements (see following section). Cumulative specific respiration (CSR) was then calculated by summing the

mass of CO_2-C respired during previous time periods and normalizing by the mass of organic C in the soil sample.

CSR data were converted to units of g CO_2-C (g C)$^{-1}$ and fitted to first-order one-, two- and three-pool decomposition models. It was found that most samples were best fit by the two-pool model with a fast-cycling and slow-cycling pool as shown in Eqn (2):

$$CSR(t) = 1 - a_{fast}e^{-k_{fast}t} - \left(1 - a_{fast}\right)e^{-k_{slow}t} \quad (2)$$

where a_{fast} is the proportion of organic C in the fast-cycling pool (unitless), k_{fast} is the decomposition rate of the fast-cycling pool (d^{-1}), k_{slow} is the decomposition rate of the slow-cycling pool (d^{-1}), and t is the time elapsed since the start of the incubation (d). Model fitting was conducted via non-linear least squares using MATLAB R2018b (MathWorks, Natick, MA, USA).

Predictor variables

To include broad-scale, distal controls in the suite of potential predictors used in our statistical analysis, several site-specific climate-related variables were compiled. Site-specific mean annual temperature and mean summer temperature were based on 30-year normals (1981-2010) from the PRISM Climate Group (PRISM Climate Group, 2019). Mean annual precipitation (MAP) was based on site-specific data available for each NEON site (NEON, 2019b). Potential evapotranspiration (PET) was based on Kramer and Chadwick (2018). Potential evapotranspiration ratio was calculated by dividing PET by MAP.

A suite of chemical analyses were conducted to characterize the chemical properties of the soil relevant to SOM dynamics. Soil pH was measured following standard procedures using a 1:1 soil-water mixture. Ammonium acetate and potassium chloride extractions were conducted at

the Oregon State University Central Analytical Laboratory (Soil Survey Staff, 2014). Selective dissolution analyses (ammonium oxalate, dithionite-citrate, and sodium pyrophosphate) were conducted following standard USDA NRCS protocols (Soil Survey Staff, 2014). Land cover, which is not included in Fig. 2.2 because it is a binary variable, was classified as either "forest" or "non-forest" based on the dominant vegetation at each site.

Several analyses were conducted to determine the quantity of C and N and the distribution of C in the soil samples. Non-incubated soil samples were density fractionated to separate three distinct fractions: the free light fraction (FLF), the occluded fraction (OCC), and the heavy fraction (HF). Density fractions were separated using sodium polytungstate and sonication following standard procedures (Strickland & Sollins, 1987; Swanston et al., 2005). Carbon content and distribution of carbon among density fractions was determined based on manometric C content. Bulk soil %N and %C were measured using an elemental analyzer (Elementar vario MAX CNS analyzer; Elementar Americas Inc., Ronkonkoma, NY, USA). Bulk soil $\delta^{13}C$ was measured using an EA-IRMS (IsoPrime 100 EA-IRMS; Isoprime Ltd, Cheadle, UK) with samples containing carbonates (those having a "k" horizon suffix) being acidified by fumigation with HCl prior to analysis (Harris, Horwáth, & van Kessel, 2001). Headspace $^{13}CO_2$ samples were taken at four intervals throughout the incubation for samples with carbonates and analyzed at the Cornell Isotope Laboratory using an IRMS (Delta V Advantage IRMS; ThermoFisher Scientific, Waltham, MA, USA).

Pyrogenic C was characterized through the analysis of benzenepolycarboxlyic acids (BPCA), which were measured on a gas chromatograph-mass spectrometer (GC-MS) following standard procedures. Three separate BPCA data products were generated by normalizing BPCA quantity by total soil mass, normalizing BPCA quantity by total soil organic C, and determining

the ratio of B6CA quantity to total BPCA quantity, which is a measure of the degree of thermal alteration of the pyrogenic C.

Statistical analysis

To determine important predictors related to SOM decomposition across continental-scale gradients, a multiple linear regression (MLR) model was built for each of the following response variables: CSR after 52 weeks ($CSR_{0\text{-}52\ wks}$), k_{fast}, and k_{slow}. Due to the differences between A and B horizons, a separate model was built for each horizon type for each response variable. Additionally, some of the responses were transformed by either taking the natural log or square root of the response to meet the assumptions of MLR. Furthermore, bulk soil %C was excluded from the list of potential predictors because of its inclusion in the calculation of CSR.

Because the number of potential predictors (p = 44) far exceeded the number of observations (n = 20) for each horizon and a number of potential predictors were correlated, a modified version of least absolute shrinkage and selection operator (LASSO) regression based on the function 'cv.glmnet' in the R package *glmnet* was used to select the largest group of predictors that yielded a mean square error (MSE) within one standard error of the minimum MSE. Since this is a machine learning algorithm that randomly partitions the data and is hence dependent on the starting seed, the LASSO procedure was repeated a total of 100 times. Variables that were selected at least 51 times were then used in best subsets regression carried out with 'regsubsets' in the R package *leaps*, and the model with the lowest Bayesian information criterion (BIC) was selected. Non-significant ($P > 0.05$) predictors were removed one at a time based on largest P-value until all remaining predictors were significant.

Results

Incubation and model fitting

Cumulative specific respiration (CSR) and decomposition rates fitted using a two-pool model (k_{fast} and k_{slow}) are summarized in Table 2.2. CSR ranged from 289 to 1716 μg CO_2-C (g C)$^{-1}$ for A horizons and from 139 to 2369 μg CO_2-C (g C)$^{-1}$ for B horizons. For A horizons, k_{fast} ranged from 1.36e-05 to 1.38e-01 d^{-1}, and it ranged from 7.07e-05 to 3.55e-01 d^{-1} for B horizons. A horizons had k_{slow} values that ranged from 3.52e-07 to 3.70e-06 d^{-1}, and B horizons had k_{slow} values that ranged from 2.22e-14 to 6.13e-06 d^{-1}. To allow for the assessment of correlations between response variables ($CSR_{0\text{-}52\ wks}$, k_{fast}, and k_{slow}) and individual predictors, Spearman's rank correlation coefficient (ρ) was calculated for each response-predictor combination (Fig. 2.2).

Table 2.2 Cumulative specific respiration (CSR) over the course of a 52-week incubation and decomposition rates based on fitting a two-pool model to the CSR data by site and horizon (k_{fast} is the fast-cycling pool decomposition rate, k_{slow} is the slow-cycling pool decomposition rate). Site-horizon combinations for which sufficient ancillary data was not available for inclusion in the MLR analysis are indicated by a dash (-).

	A Horizons				B Horizons			
Site	Horizon	$CSR_{0\text{-}52\ wks}$ (μg CO_2-C (g C)$^{-1}$)	k_{fast} (d^{-1})	k_{slow} (d^{-1})	Horizon	$CSR_{0\text{-}52\ wks}$ (μg CO_2-C (g C)$^{-1}$)	k_{fast} (d^{-1})	k_{slow} (d^{-1})
ABBY	-	-	-	-	Bt1	186	2.98E-02	3.78E-07
BLAN	Ap1	1467	1.38E-01	2.84E-06	Bt1	951	1.32E-01	1.94E-06
CLBJ	A1	1716	4.71E-02	3.70E-06	Bt1	651	3.32E-03	2.22E-14
CPER	A1	1475	8.16E-02	3.13E-06	Bw1	2369	2.63E-01	6.13E-06
DCFS	A1	652	5.48E-02	1.08E-06	Bw1	692	3.29E-01	1.36E-06
DSNY	A	1171	1.36E-05	2.63E-06	Bh1	547	1.02E-04	1.42E-06
GRSM	A	365	8.62E-02	6.69E-07	Bt1	390	3.55E-01	1.02E-06
JORN	Ak	1367	1.47E-02	1.66E-06	-	-	-	-
KONA	Ap	482	9.32E-02	8.92E-07	Bt1	250	5.09E-02	3.08E-07
KONZ	A1	885	4.25E-02	1.42E-06	Bt1	701	1.73E-02	9.13E-07
MOAB	A	1294	8.49E-03	1.11E-06	-	-	-	-
NGPR	A	994	3.41E-02	1.85E-06	Bt1	496	7.86E-02	1.07E-06
NIWO	A	289	1.55E-02	3.52E-07	Bw1	139	2.22E-02	2.29E-07
OSBS	A	699	4.03E-02	1.16E-06	Bw1	834	1.29E-03	2.22E-14
RMNP	A1	883	1.38E-02	1.12E-06	Bt	717	9.74E-04	2.22E-14
SERC	A	917	5.04E-02	1.64E-06	Bt1	1481	7.07E-05	3.79E-06
SJER	A	1090	6.96E-03	4.10E-07	Bw1	610	3.27E-02	1.11E-06
SOAP	A	655	2.89E-02	1.19E-06	Bt1	370	6.57E-02	7.95E-07
STER	-	-	-	-	Bkt1	498	3.01E-01	1.18E-06
TALL	A1	812	1.27E-02	6.45E-07	Bt1	712	2.95E-04	1.91E-06
UNDE	A	726	2.89E-02	8.72E-07	Bhs	239	2.71E-02	3.81E-07
WOOD	Apk	1264	2.67E-02	2.50E-06	Bk1	661	5.10E-04	1.75E-06

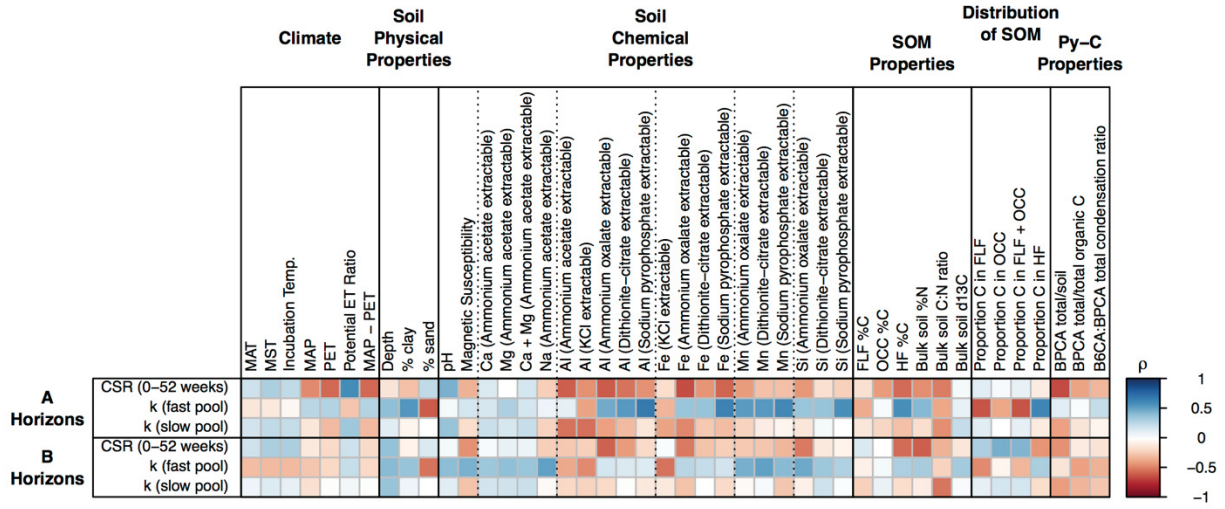

Fig. 2.2 Correlation plot showing Spearman's rank correlation coefficient (ρ) for three response metrics (CSR from 0 to 52 weeks, k_{fast}, and k_{slow}) by horizon. Correlation coefficients and corresponding P-values are given in Appendix A.

Py-C, pyrogenic C; MAT, mean annual temperature; MST, mean summer temperature; MAP, mean annual precipitation; PET, potential evapotranspiration; Potential ET Ratio = PET/MAP; FLF, free light fraction; OCC, occluded fraction; HF, heavy fraction; BPCA, benzenepolycarboxlyic acids

Cumulative specific respiration

CSR was calculated for the entire duration of the 52-week incubation as well as for the first half (0 to 26 weeks) and second half (26 to 52 weeks) of the incubation. Due to non-normality, the Wilcoxon rank sum test was used to test for significant differences between A and B horizons. CSR from 0 to 52 weeks in A horizons was significantly higher ($P = 0.009$) than CSR from 0 to 52 weeks in B horizons (Fig. 2.3a). CSR was also significantly higher in A horizons from 0 to 26 weeks ($P < 0.001$, Fig 2.3b). However, CSR was not significantly different ($P = 0.678$) between A and B horizons from 26 to 52 weeks (Fig. 2.3c).

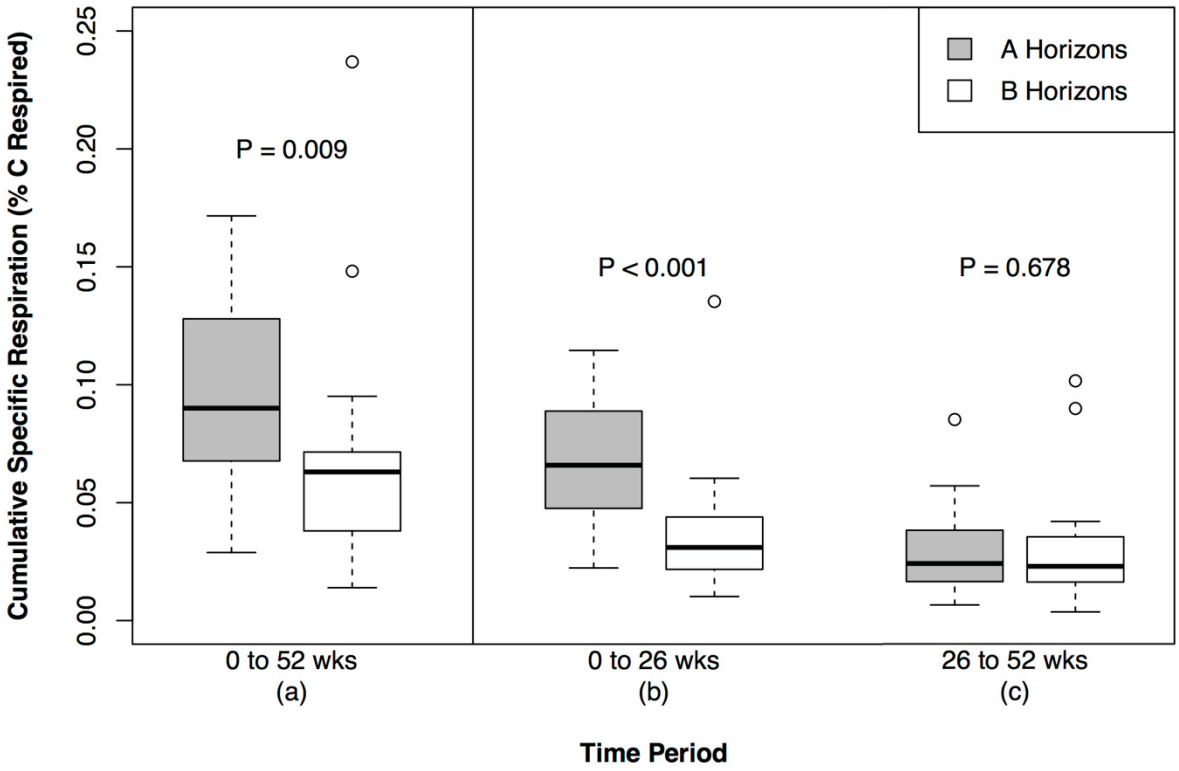

Fig. 2.3 Box plot of CSR by time period and horizon. P-values correspond to the Wilcoxon rank sum test between the two horizons for a given time interval.

The final MLR model for A horizon CSR had an R^2 of 0.86 (Table 2.3). ΔR^2 values were used to express the amount of unique variance explained by each predictor, and the directionality of the effect of each predictor are indicated by (+) for a positive effect and (-) for a negative effect. The significant predictors ($P \leq 0.05$) in order of relative importance according to ΔR^2 values are ammonium oxalate extractable Fe (-), bulk soil C:N ratio (-), and dithionite-citrate extractable Si (-) (Table 2.3). For B horizon CSR, an R^2 value of 0.75 was achieved with the final model (Table 2.3). Significant predictors in order of ΔR^2 relative importance are proportion

of organic C in the occluded fraction (+), ammonium oxalate extractable Fe (-), and total benzenepolycarboxylic acids (BPCA) normalized by soil mass (-) (Table 2.3).

Table 2.3 Multiple linear regression (MLR) results for CSR over 52 weeks by horizon. Note that only significant ($P \leq 0.05$) predictors were included in the model. To meet the assumptions of MLR, the response was log transformed for B horizon samples.

Horizon | Response	Coefficients	Estimate	S.E.	D.F.	t statistic	p-value	$\Delta R^{2\dagger}$
A | $CSR_{0\text{-}52\ wks}$	Intercept	2001.04	127.91	3, 16	15.64	< 0.001	N/A
	Ammonium oxalate extractable Fe	-1697.14	197.99	3, 16	-8.57	< 0.001	0.63
	Bulk soil C:N ratio	-27.24	4.43	3, 16	-6.15	< 0.001	0.32
	Dithionite-citrate extractable Si	-3019.14	759.25	3, 16	-3.98	0.001	0.14
						Total Model R^2:	0.86
B | ln($CSR_{0\text{-}52\ wks}$)	Intercept	6.35	0.17	3, 16	36.35	< 0.001	N/A
	Proportion org. C in OCC	3.56	0.79	3, 16	4.48	< 0.001	0.31
	Ammonium oxalate extractable Fe	-1.27	0.40	3, 16	-3.16	0.006	0.16
	Total BPCA/soil	-1.07	0.40	3, 16	-2.68	0.017	0.11
						Total Model R^2:	0.75

$^{\dagger}\Delta R^2$ values express the unique variance explained by a predictor and do not necessarily sum to total model R^2

CSR, cumulative specific respiration; OCC, occluded fraction; BPCA, benzenepolycarboxylic acids

Decomposition rates

Pool-specific decomposition rates (k_{fast} and k_{slow}) were compared between A and B horizons using the Wilcoxon rank sum test due to non-normality (Fig. 2.4). There were no significant differences between horizons for k_{fast} (Fig. 2.4a) or for k_{slow} (Fig. 2.4b).

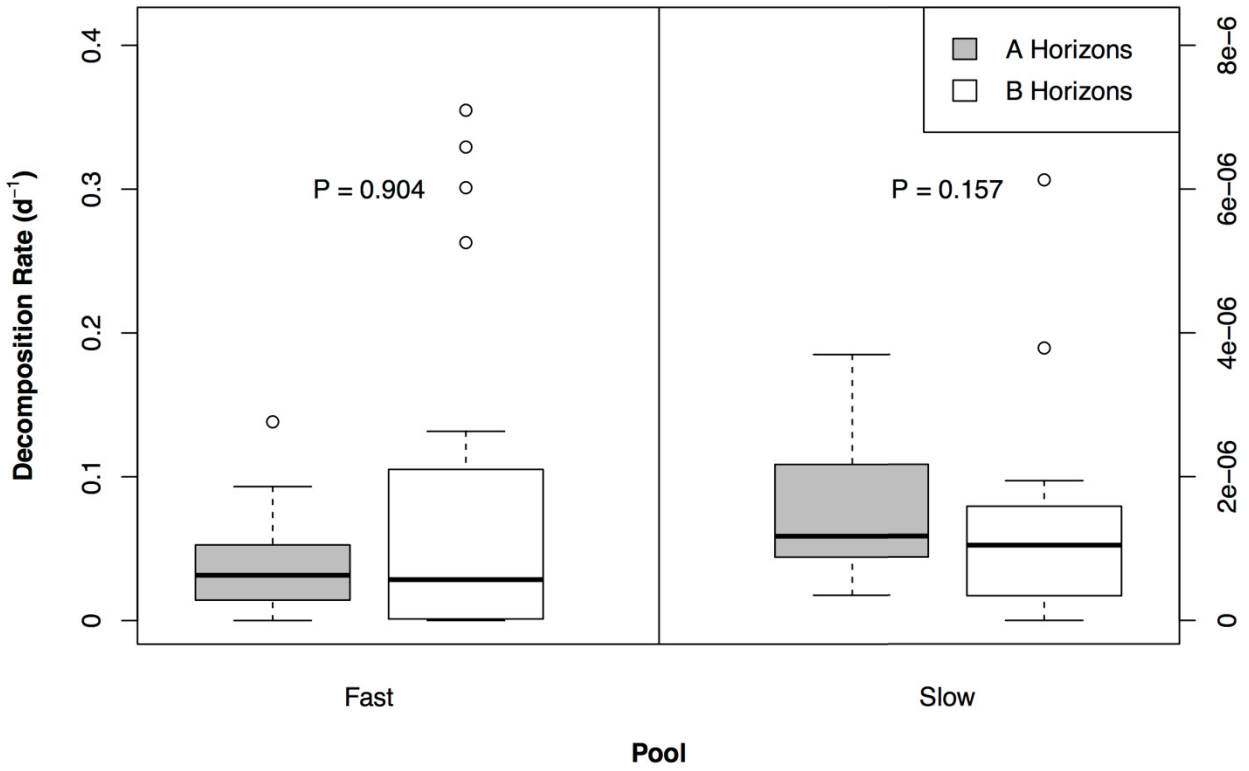

Fig. 2.4 Box plot of decomposition rate (*k*) by pool and horizon. P-values correspond to the Wilcoxon rank sum test between horizons for a given decomposition rate.

For k_{fast}, the final MLR model R^2 value achieved for A horizons was 0.74 (Table 2.4). Significant predictors for k_{fast} in A horizons in order of relative importance according to ΔR^2 values are sodium pyrophosphate extractable Mn (+), non-forest land cover (+), total BPCA normalized by soil mass (-), and mean annual precipitation (+) (Table 2.4). For k_{fast} in B horizons, the final model had an R^2 value of 0.69 (Table 2.4). Significant predictors for B horizon k_{fast} values in order of ΔR^2 importance are depth (+), bulk soil %N (+), and total BPCA normalized to total soil organic C (-) (Table 2.4).

Table 2.4 MLR results for fitted fast pool decomposition rate (k_{fast}) by horizon. Note that only significant ($P \leq 0.05$) predictors were included in the model. To meet the assumptions of MLR, a square root transformation was applied to the response for both horizons.

Horizon | Response	Coefficients	Estimate	S.E.	D.F.	t statistic	p-value	$\Delta R^{2\dagger}$
A | sqrt(k_{fast})	Intercept	0.00	0.04	4, 15	-0.07	0.942	N/A
	Sodium pyrophosphate extractable Mn	5.87	1.14	4, 15	5.16	< 0.001	0.45
	Land cover (non-forest)	0.11	0.03	4, 15	3.81	0.002	0.25
	MAP	1.26E-04	3.92E-05	4, 15	3.22	0.006	0.18
	Total BPCA/soil	-0.11	0.03	4, 15	-3.18	0.006	0.17
					Total Model R^2:		0.74
B | sqrt(k_{fast})	Intercept	-1.46E-01	9.53E-02	3, 16	-1.53	0.146	N/A
	$(Depth)^2$	2.01E-04	4.08E-05	3, 16	4.92	< 0.001	0.46
	Bulk soil %N	4.20E+00	1.13E+00	3, 16	3.72	0.002	0.26
	Total BPCA/total organic C	-6.78E-03	1.85E-03	3, 16	-3.66	0.002	0.26
					Total Model R^2:		0.69

$^{\dagger}\Delta R^2$ values express the unique variance explained by a predictor and do not necessarily sum to total model R^2

BPCA, benzenepolycarboxylic acids; MAP, mean annual precipitation

For k_{slow}, the final model for A horizons had an R^2 of 0.66 (Table 2.5). Significant predictors for A horizon k_{slow} values in order of relative importance according to ΔR^2 values are ammonium oxalate extractable Fe (-), KCl extractable Fe (-), and potential evapotranspiration ratio (-) (Table 2.5). For B horizons, the final model for k_{slow} had an R^2 of 0.41 (Table 2.5). Significant predictors for k_{slow} in B horizons in order of ΔR^2 importance are bulk soil C:N ratio (-) and proportion of organic C in the occluded fraction (+).

Table 2.5 MLR results for fitted slow pool decomposition rate (k_{slow}) by horizon. Note that only significant ($P \leq 0.05$) predictors were included in the model. To meet the assumptions of MLR, a log transformation was applied to the A horizon response, and a square root transformation was applied to the B horizon response.

Horizon | Response	Coefficients	Estimate	S.E.	D.F.	t statistic	p-value	$\Delta R^{2\dagger}$
A | ln(k_{slow})	Intercept	-12.79	0.20	3, 16	-65.11	< 0.001	N/A
	Ammonium oxalate extractable Fe	-2.44	0.60	3, 16	-4.06	< 0.001	0.35
	ln(KCl extractable Fe)	-0.63	0.16	3, 16	-3.99	0.001	0.34
	ln(PET ratio)	-0.46	0.16	3, 16	-2.83	0.012	0.17
						Total Model R^2:	0.66
B | sqrt(k_{slow})	Intercept	1.32E-03	2.82E-04	2, 17	4.69	< 0.001	N/A
	Bulk soil C:N ratio	-4.03E-05	1.45E-05	2, 17	-2.78	0.013	0.27
	Proportion org. C in OCC	2.80E-03	1.08E-03	2, 17	2.59	0.019	0.23
						Total Model R^2:	0.41

$^{\dagger}\Delta R^2$ values express the unique variance explained by a predictor and do not necessarily sum to total model R^2

PET ratio, potential evapotranspiration ratio = PET/MAP; OCC, occluded fraction

Discussion

Controls on cumulative specific respiration

Based on the results of the MLR model selection procedure for CSR, there are two controls on CSR common to both A and B horizons in our continental-scale sample set: non-crystalline minerals and soil organic matter (SOM) chemistry. Ammonium oxalate extractable Fe, which is a measure of Fe-bearing non-crystalline minerals in a soil sample (Soil Survey Staff, 2014), was a significant predictor for CSR in both A and B horizons and had a negative effect on CSR in both horizons (Table 2.3). Additionally, in A horizons, dithionite-citrate extractable Si, a metric of the quantity of amorphous aluminosilicates (Wada, 1989), had a significant negative effect on CSR. Because LASSO regression selects a suite of non-correlated predictors that

maximizes explanatory power and excludes all other variables (including relevant but correlated variables), the variables selected should generally be interpreted as representing a group of predictors indicative of a given mechanism. Consequently, the selection of ammonium oxalate extractable Fe instead of ammonium oxalate extractable Al, which quantifies the abundance of allophane, imogolite, and other Al-containing non-crystalline minerals (Wada, 1989), does not necessarily mean that Fe-bearing non-crystalline minerals have a stronger effect on SOM decomposition than Al-bearing non-crystalline minerals. Instead, the selection of ammonium oxalate extractable Fe as a significant predictor indicates the importance of non-crystalline minerals in general in regulating SOM decomposition. This finding is consistent with a number of studies that have demonstrated the importance of non-crystalline minerals in controlling SOM decomposition (Doetterl et al., 2015; Rasmussen, Southard, & Horwath, 2006; Torn, Trumbore, Chadwick, Vitousek, & Hendricks, 1997b), which is attributed to SOM adsorption to and co-precipitation with non-crystalline minerals (Kleber et al., 2015).

The specific mechanism by which SOM chemistry influenced CSR varied by horizon. For A horizons, CSR decreased with increasing bulk soil C:N ratio, whereas in B horizons, total BPCA normalized by soil mass had a negative effect on CSR (Table 2.3). Consistent with these results, numerous decomposition studies have shown the importance of substrate chemistry (e.g., Melillo, Aber, & Muratore, 1982) in controlling decomposition. Both non-crystalline minerals and SOM chemistry could explain the temporal trend in the differences in CSR between horizons. From 0 to 26 weeks, CSR significantly differed between A and B horizons (Fig. 2.3b); however, CSR was not significantly different between horizons from 26 to 52 weeks (Fig. 2.3c). During the first 26 weeks of the incubation, CSR was most likely dominated by the decomposition of relatively labile particulate matter in the free light fraction (Collins et al., 2000;

Townsend, Vitousek, Desmarais, & Tharpe, 1997), resulting in CSR being higher for A horizons. This is consistent with the proportion of C in the fast-cycling pool being significantly higher ($P = 0.006$) in A horizons in our sample set and with the findings of Schrumpf *et al.* (2013), who found specific respiration decreased with depth during a 20-day incubation. However, after 26 weeks, this labile pool had likely been largely exhausted (Conant et al., 2008; Emerson, Roden, & Twining, 2012; Xu, Zhou, Ruan, Luo, & Wang, 2010), and consequently, from 26 to 52 weeks, CSR was more representative of the decomposition of stable SOM (Townsend et al., 1997), including SOM stabilized via organo-mineral associations as well as more chemically complex SOM, which should result in a smaller difference in CSR between horizons.

The only noticeably different predictor of CSR between horizons was the proportion of organic C in the occluded fraction (Table 2.3), and this is most likely an artifact of the sample preparation process for the incubation. Mean residence times of SOM in the occluded fraction generally are between the mean residence times of SOM in the free light fraction and SOM in the heavy fraction, and consequently, occluded fraction SOM is typically viewed as having at least some protection from microbial degradation (Schrumpf et al., 2013; Swanston et al., 2005). However, due to the sonication involved in separating the occluded fraction from the heavy fraction, artifacts can potentially be introduced, such as the inclusion of roots (Schrumpf et al., 2013) or organo-mineral associations (Kaiser & Guggenberger, 2007) in the occluded fraction. Consequently, since the directionality of the effect of the proportion of organic C in the occluded fraction is opposite of what would be expected, it is likely that some fine roots partly associated with aggregates were included in this fraction for at least some samples. Given that bulk soil C concentrations are generally lower in B horizons than A horizons (0.7% C in B horizons vs. 2.2

%C in A horizons in this study), the inclusion of roots would have an outsized influence in B horizon samples as compared to A horizon samples.

Controls on decomposition rates

As with CSR, SOM chemistry appears to be a common control on the fast-cycling pool decomposition rate (k_{fast}) in both A horizons and B horizons. Increased quantities of BPCA were associated with a decrease in k_{fast} in both horizons, while bulk soil %N was associated with an increase in k_{fast} in B horizons (Table 2.4). As with CSR, the effect of SOM chemistry on decomposition rates is consistent with numerous studies (e.g., Melillo et al., 1982). What is particularly interesting, however, is the influence of pyrogenic C on fast pool decomposition rates in both A and B horizons. Until recently, pyrogenic C was thought to be highly resistant to decomposition and have mean residence times on the order of millennia (Bird, Wynn, Saiz, Wurster, & McBeath, 2015; Kuzyakov, Subbotina, Chen, Bogomolova, & Xu, 2009); however, numerous studies have confirmed that a substantial fraction of pyrogenic C is vulnerable to biological degradation (De La Rosa, Miller, & Knicker, 2018; Hilscher, Heister, Siewert, & Knicker, 2009; Hilscher & Knicker, 2011), resulting in mean residence times on the scale of decades to centuries (Hilscher et al., 2009; Santos, Torn, & Bird, 2012). Fitting a two-pool model to 177-day incubation data, Cheng, Lehmann, Thies, & Burton (2008) found that soils with pyrogenic C from historical charcoal blast furnace sites had lower k_{fast} and k_{slow} values than soils from adjacent sites without pyrogenic C, which agrees with our finding of increased quantities of pyrogenic C having a negative effect on k_{fast}. Our findings are also consistent with a number of biochar amendment incubation studies that found a sustained decrease in SOM decomposition rates after a transient initial increase in SOM decomposition (Whitman, Zhu, & Lehmann, 2014;

Zimmerman, Gao, & Ahn, 2011). Together, this evidence suggests that pyrogenic C exerts a strong influence on the rate at which the fast pool decomposes.

Unlike CSR, there are a number of differences between predictors of k_{fast} in A and B horizons. Sodium pyrophosphate extractable Mn had a positive effect on k_{fast} in A horizons (Table 2.4). This is consistent with findings of enhanced forest floor litter decomposition with higher concentrations of Mn (Berg, Steffen, & McClaugherty, 2007; Keiluweit et al., 2015). Using a suite of chemical imaging methods, Keiluweit *et al.* (2015) showed that Mn^{2+} is scavenged by fungi and then converted to Mn^{3+} species to oxidize litter as part of the decomposition process. Given the relatively large proportion of C in the free light fraction in A horizons in this sample set (the mean percentage of organic C in the free light fraction in A horizons was 30.7%), it is plausible that similar Mn redox cycling is a primary driver of the decomposition of unprotected particulate organic matter in A horizons. Additionally, land cover (i.e., forest vs. non-forest) and mean annual precipitation are significant predictors for k_{fast} in A horizons but not in B horizons. These results are consistent with other studies that have found that the influence of climate and/or vegetation cover on SOC stocks decrease with depth (Gray, Bishop, & Wilson, 2015; Jobbagy & Jackson, 2000). Consequently, this suggests that A horizons are more heavily influenced by external controls given their closer proximity to the surface. In contrast, depth was a significant predictor only for B horizons. This can be explained by the greater variability in horizon depth for B horizons than A horizons used in this study.

In contrast to k_{fast}, there were no significant predictors of the slow-cycling pool decomposition rate (k_{slow}) common to both A and B horizons. Ammonium oxalate extractable Fe, KCl extractable Fe, and potential evapotranspiration (PET) ratio (PET/MAP) were significant predictors for k_{slow} in A horizons (Table 2.5). The inclusion of ammonium oxalate extractable Fe

as a control on the decomposition rate of the slow-cycling pool in A horizons is consistent with the negative effect of non-crystalline minerals on CSR. Additionally, the inclusion of a climate-related metric, PET ratio, is consistent with climate having a larger influence on A horizons than B horizons as stated above for k_{fast}. Significant predictors of k_{slow} in B horizons were bulk soil C:N ratio and the proportion of organic C in the occluded fraction (Table 2.5). The negative effect of bulk soil C:N ratio on the decomposition rate of the slow pool in B horizons is consistent with the positive effect of bulk soil %N k_{fast} in B horizons. This suggests that SOM decomposition in B horizons may generally be at least in part N limited. This is consistent with the results of several laboratory incubation studies that have found that the addition of N increased decomposition rates in B horizons but not A horizons (Fierer, Allen, Schimel, & Holden, 2003; Tian et al., 2016). As with CSR, the positive effect of the proportion of organic C in the occluded fraction on k_{slow} is likely an experimental artifact related to the potential accidental inclusion of fine roots in the incubated samples.

It is interesting to note that despite different predictors being returned as significant for the different decomposition rates in A and B horizons, there were no significant differences between decomposition rates between A and B horizons (Fig. 2.4). Furthermore, it is somewhat surprising that incubation temperature was never returned as a significant predictor of either pool-specific decomposition rate, which suggests that proximal controls overwhelm any effect of temperature on decomposition rate.

Implications for predicting SOM decomposition at a continental scale

The important role of non-crystalline minerals in regulating SOM decomposition as indicated by the inclusion of ammonium oxalate extractable Fe as a significant predictor instead

of % clay for CSR in both horizons and k_{slow} in A horizons is consistent with the emerging understanding of the need to move beyond the use of clay as a proxy for SOM mineral stabilization in Earth system models (ESMs) (Rasmussen et al., 2018). Given that it has been suggested that organo-mineral associations are the most important mechanism for long-term SOM stabilization (Schrumpf et al., 2013; M. von Lützow et al., 2006), accurately representing mineral-associated SOM in ESMs is critical for predicting terrestrial carbon-climate feedbacks as well as optimizing land management to sequester C to mitigate climate change. A potential avenue for future research is to incorporate data related to the distribution of non-crystalline minerals from existing data sources, such as the USDA NRCS Soil Survey Geographic Database (SSURGO), into sub-models of SOM decomposition in ESMs.

The role played by N as a predictor of several response metrics in this study, represented either as bulk soil C:N ratio or bulk soil %N, suggests that changes in the N status of a system through altered N inputs could potentially enhance SOM decomposition, particularly in subsurface soils. This apparently contradicts the large body of literature that suggests increased N inputs decreases SOM decomposition rates as microbial community composition shifts to phyla that favor the decomposition of more labile substrates (Cusack, Torn, Mcdowell, & Silver, 2010; Frey et al., 2014; Ramirez, Craine, & Fierer, 2012). However, this body of literature is largely based on work focusing on the top 10 cm of soil; in contrast, Fierer *et al.* (2003) and Tian *et al.* (2016) included soil samples from below 30 cm in their laboratory incubation nutrient addition experiments and did find a positive effect of N addition on SOM decomposition. Consequently, it cannot be assumed that SOM in B horizons will respond to nutrient additions in the same way as SOM in A horizons, and the net effect of increased N inputs to a system may

depend on the balance between decreased SOM decomposition in A horizons and increased SOM decomposition in B horizons.

Using data from a 52-week laboratory incubation of a soil sample set spanning the conterminous United States and fitting a two-pool decomposition model to the incubation data, this study provides evidence for the dominant role played by proximal controls in predicting SOM decomposition at a continental scale. Non-crystalline minerals and SOM chemistry were significant predictors of CSR, a metric of SOM vulnerability to decomposition, in both A and B horizons. Predictors of decomposition rates derived using the two-pool model were more diverse. Fast-cycling pool decomposition rates in both horizons were related to an index of pyrogenic C, whereas B horizon decomposition rates were largely controlled by the amount of N in the sample. The results from this study support the acknowledged need for using a more mechanistically-relevant proxy other than clay for mineral-associated SOM in ESMs, and they show the importance of considering the effects of changes in N inputs in addition to changes in climate on SOM decomposition rates.

Acknowledgements

This study was funded by the U.S. National Science Foundation under awards EF-1340681 and DBI-1724433. The authors would like to acknowledge the National Ecological Observatory Network Systems Installation and Verification Team for the collection of soil cores and Stephanie Duston and Dave Mitchem for assistance with laboratory work.

References

Berg, B., Steffen, K. T., & McClaugherty, C. (2007). Litter decomposition rate is dependent on litter Mn concentrations. *Biogeochemistry*, *82*(1), 29–39.

Bird, M. I., Wynn, J. G., Saiz, G., Wurster, C. M., & McBeath, A. (2015). The Pyrogenic Carbon Cycle. *Annual Review of Earth and Planetary Sciences*, *43*(1), 273–298.

Burke, I. C., Yonker, C. M., Parton, W. J., Cole, C. V., Schimel, D. S., & Flach, K. (1989). Texture, Climate, and Cultivation Effects on Soil Organic Matter Content in U.S. Grassland Soils. *Soil Science Society of America Journal*, *53*(3), 800.

Cheng, C. H., Lehmann, J., Thies, J. E., & Burton, S. D. (2008). Stability of black carbon in soils across a climatic gradient. *Journal of Geophysical Research: Biogeosciences*, *113*(2), 1–10.

Collins, H. P., Elliott, E. T., Paustian, K., Bundy, L. G., Dick, W. A., Huggins, D. R., … Paul, E. A. (2000). Soil carbon pools and fluxes in long-term Corn Belt agroecosystems. *Soil Biology and Biochemistry*, *32*(2), 157–168.

Conant, R. T., Drijber, R. A., Haddix, M. L., Parton, W. J., Paul, E. A., Plante, A. F., … Steinweg, M. J. (2008). Sensitivity of organic matter decomposition to warming varies with its quality. *Global Change Biology*, *14*(4), 868–877.

Cusack, D. F., Torn, M. S., Mcdowell, W. H., & Silver, W. L. (2010). The response of heterotrophic activity and carbon cycling to nitrogen additions and warming in two tropical soils. *Global Change Biology*, *16*(9), 2555–2572.

De La Rosa, J. M., Miller, A. Z., & Knicker, H. (2018). Soil-borne fungi challenge the concept of long-term biochemical recalcitrance of pyrochar. *Scientific Reports*, *8*(1), 2896.

Doetterl, S., Stevens, A., Six, J., Merckx, R., Van Oost, K., Casanova Pinto, M., … Boeckx, P.

(2015). Soil carbon storage controlled by interactions between geochemistry and climate. *Nature Geoscience*, *8*(10), 780–783.

Dungait, J. A. J., Hopkins, D. W., Gregory, A. S., & Whitmore, A. P. (2012). Soil organic matter turnover is governed by accessibility not recalcitrance. *Global Change Biology*, *18*(6), 1781–1796.

Emerson, D., Roden, E., & Twining, B. S. (2012). The microbial ferrous wheel: Iron cycling in terrestrial, freshwater, and marine environments. *Frontiers in Microbiology*, *3*(SEP), 383.

Fierer, N., Allen, A. S., Schimel, J. P., & Holden, P. A. (2003). Controls on microbial CO 2 production: A comparison of surface and subsurface soil horizons. *Global Change Biology*, *9*(9), 1322–1332.

Frey, S. D., Ollinger, S., Nadelhoffer, K., Bowden, R., Brzostek, E., Burton, A., … Wickings, K. (2014). Chronic nitrogen additions suppress decomposition and sequester soil carbon in temperate forests. *Biogeochemistry*, *121*(2), 305–316.

Friedlingstein, P., Cox, P., Betts, R., Bopp, L., von Bloh, W., Brovkin, V., … Zeng, N. (2006). Climate–Carbon Cycle Feedback Analysis: Results from the C 4 MIP Model Intercomparison. *Journal of Climate*, *19*(14), 3337–3353.

Friedlingstein, P., Meinshausen, M., Arora, V. K., Jones, C. D., Anav, A., Liddicoat, S. K., … Knutti, R. (2014). Uncertainties in CMIP5 Climate Projections due to Carbon Cycle Feedbacks. *Journal of Climate*, *27*(2), 511–526.

Gray, J. M., Bishop, T. F. A., & Wilson, B. R. (2015). Factors Controlling Soil Organic Carbon Stocks with Depth in Eastern Australia. *Soil Science Society of America Journal*, *79*(6), 1741.

Harris, D., Horwáth, W. R., & van Kessel, C. (2001). Acid fumigation of soils to remove

carbonates prior to total organic carbon or CARBON-13 isotopic analysis. *Soil Science Society of America Journal*, *65*(6), 1853.

Hilscher, A., Heister, K., Siewert, C., & Knicker, H. (2009). Mineralisation and structural changes during the initial phase of microbial degradation of pyrogenic plant residues in soil. *Organic Geochemistry*, *40*(3), 332–342.

Hilscher, A., & Knicker, H. (2011). Carbon and nitrogen degradation on molecular scale of grass-derived pyrogenic organic material during 28 months of incubation in soil. *Soil Biology and Biochemistry*, *43*(2), 261–270.

Jobbagy, E. G., & Jackson, R. B. (2000). The vertical distribution of soil organic carbon and its relation to climate and vegetation. *Ecological Applications*, *10*(2), 423–436.

Kaiser, K., & Guggenberger, G. (2007). Distribution of hydrous aluminium and iron over density fractions depends on organic matter load and ultrasonic dispersion. *Geoderma*, *140*(1–2), 140–146.

Keiluweit, M., Nico, P., Harmon, M. E., Mao, J., Pett-Ridge, J., & Kleber, M. (2015). Long-term litter decomposition controlled by manganese redox cycling. *Proceedings of the National Academy of Sciences of the United States of America*, *112*(38), E5253-60.

Kleber, M., Eusterhues, K., Keiluweit, M., Mikutta, C., Mikutta, R., & Nico, P. S. (2015). Mineral-Organic Associations: Formation, Properties, and Relevance in Soil Environments. *Advances in Agronomy*, *130*, 1–140.

Köchy, M., Hiederer, R., & Freibauer, A. (2015). Global distribution of soil organic carbon – Part 1: Masses and frequency distributions of SOC stocks for the tropics, permafrost regions, wetlands, and the world. *SOIL*, *1*(1), 351–365.

Kramer, M. G., & Chadwick, O. A. (2018). Climate-driven thresholds in reactive mineral

retention of soil carbon at the global scale. *Nature Climate Change*, *8*(12), 1104–1108.

Kuzyakov, Y., Subbotina, I., Chen, H., Bogomolova, I., & Xu, X. (2009). Black carbon decomposition and incorporation into soil microbial biomass estimated by 14C labeling. *Soil Biology and Biochemistry*, *41*(2), 210–219.

Le Quéré, C., Andrew, R., Friedlingstein, P., Sitch, S., Hauck, J., Pongratz, J., … Zheng, B. (2018). Global Carbon Budget 2018. *Earth System Science Data*, *10*(4), 2141–2194.

Lehmann, J., & Kleber, M. (2015). The contentious nature of soil organic matter. *Nature*, *528*, 60–68.

Lloyd, J., & Taylor, J. A. (1994). On the Temperature Dependence of Soil Respiration. *Functional Ecology*, *8*(3), 315.

Melillo, J. M., Aber, J. D., & Muratore, J. F. (1982). Nitrogen and Lignin Control of Hardwood Leaf Litter Decomposition Dynamics. *Ecology*, *63*(3), 621–626.

NEON. (2019a). *Data Product: NEON.DP1.00096.001*. Boulder, CO, USA: Battelle.

NEON. (2019b). *Field Sites*. Boulder, CO, USA: Battelle.

Paul, E.A., Collins, H. P., & Leavitt, S. W. (2001). Dynamics of resistant soil carbon of Midwestern agricultural soils measured by naturally occurring 14C abundance. *Geoderma*, *104*(3–4), 239–256.

Paul, Eldor A., Morris, S. J., Conant, R. T., & Plante, A. F. (2006). Does the Acid Hydrolysis–Incubation Method Measure Meaningful Soil Organic Carbon Pools? *Soil Science Society of America Journal*, *70*(3), 1023.

Post, W. M., Emanuel, W. R., Zinke, P. J., & Stangenberger, A. G. (1982). Soil carbon pools and world life zones. *Nature*, *298*(5870), 156–159.

Prentice, I. C., Fasham, M. J. R., Goulden, M., Heimann, M., Jaramillo, V., Kheshgi, H., …

Farquhar, G. (2001). The carbon cycle and atmospheric carbon dioxide. In J. T. Houghton, Y. Ding, D. J. Griggs, M. Noguer, P. J. van der Linden, X. Dai, & K. M. an (Eds.), *Climate Change 2001: The Scientific Basis* (pp. 183–237). Cambridge, UK: Cambridge University Press.

PRISM Climate Group. (2019). PRISM Climate Data.

Ramirez, K. S., Craine, J. M., & Fierer, N. (2012). Consistent effects of nitrogen amendments on soil microbial communities and processes across biomes. *Global Change Biology*, *18*(6), 1918–1927.

Rasmussen, C., Heckman, K., Wieder, W. R., Keiluweit, M., Lawrence, C. R., Berhe, A. A., … Wagai, R. (2018). Beyond clay: towards an improved set of variables for predicting soil organic matter content. *Biogeochemistry*, *137*(3), 297–306.

Rasmussen, C., Southard, R. J., & Horwath, W. R. (2006). Mineral control of organic carbon mineralization in a range of temperate conifer forest soils. *Global Change Biology*, *12*(5), 834–847.

Santos, F., Torn, M. S., & Bird, J. A. (2012). Biological degradation of pyrogenic organic matter in temperate forest soils. *Soil Biology and Biochemistry*, *51*, 115–124.

Saxton, K., Rawls, W. J., Romberger, J., & Papendick, R. (1986). Estimating generalized soil-water characteristics from texture. *Soil Science Society of America Journal*, *50*(4), 1031–1036.

Schmidt, M. W. I., Torn, M. S., Abiven, S., Dittmar, T., Guggenberger, G., Janssens, I. A., … Trumbore, S. E. (2011). Persistence of soil organic matter as an ecosystem property. *Nature*, *478*(7367), 49–56.

Schrumpf, M., Kaiser, K., Guggenberger, G., Persson, T., Kögel-Knabner, I., & Schulze, E. D.

(2013). Storage and stability of organic carbon in soils as related to depth, occlusion within aggregates, and attachment to minerals. *Biogeosciences*, *10*(3), 1675–1691.

Soil Survey Staff. (2014). *Kellogg Soil Survey Laboratory Methods Manual*.

Soil Survey Staff. (2017). *Web Soil Survey*. USDA Natural Resources Conservation Service.

Sollins, P., Homann, P., & Caldwell, B. A. (1996). Stabilization and destabilization of soil organic matter: Mechanisms and controls. *Geoderma*, *74*(1–2), 65–105.

Strickland, T. C., & Sollins, P. (1987). Improved Method for Separating Light- and Heavy-Fraction Organic Material from Soil. *Soil Science Society of America Journal*, *51*(5), 1390.

Swanston, C. W., Caldwell, B. A., Homann, P. S., Ganio, L., & Sollins, P. (2002). Carbon dynamics during a long-term incubation of separate and recombined density fractions from seven forest soils. *Soil Biology and Biochemistry*, *34*(8), 1121–1130.

Swanston, C. W., Torn, M. S., Hanson, P. J., Southon, J. R., Garten, C. T., Hanlon, E. M., & Ganio, L. (2005). Initial characterization of processes of soil carbon stabilization using forest stand-level radiocarbon enrichment. *Geoderma*, *128*(1–2), 52–62.

Tarnocai, C., Canadell, J. G., Schuur, E. A. G., Kuhry, P., Mazhitova, G., & Zimov, S. (2009). Soil organic carbon pools in the northern circumpolar permafrost region. *Global Biogeochemical Cycles*, *23*(2), 1–11.

Tian, Q., Yang, X., Wang, X., Liao, C., Li, Q., Wang, M., … Liu, F. (2016). Microbial community mediated response of organic carbon mineralization to labile carbon and nitrogen addition in topsoil and subsoil. *Biogeochemistry*, *128*(1–2), 125–139.

Todd-Brown, K. E. O., Randerson, J. T., Post, W. M., Hoffman, F. M., Tarnocai, C., Schuur, E. A. G., & Allison, S. D. (2013). Causes of variation in soil carbon simulations from CMIP5 Earth system models and comparison with observations. *Biogeosciences*, *10*(3), 1717–1736.

Torn, M. S., Swanston, C. W., Castanha, C., & Trumbore, S. E. (2009). Storage and Turnover of Organic Matter in Soil. In *Biophysico-Chemical Processes Involving Natural Nonliving Organic Matter in Environmental Systems* (pp. 219–272).

Torn, M. S., Trumbore, S. E., Chadwick, O. A., Vitousek, P. M., & Hendricks, D. M. (1997). Mineral control of soil organic carbon storage and turnover. *Nature*, *389*(6647), 170–173.

Torn, M. S., Vitousek, P. M., & Trumbore, S. E. (2005). The Influence of Nutrient Availability on Soil Organic Matter Turnover Estimated by Incubations and Radiocarbon Modeling. *Ecosystems*, *8*(4), 352–372.

Townsend, A. R., Vitousek, P. M., Desmarais, D. J., & Tharpe, A. (1997). Soil carbon pool structure and temperature sensitivity inferred using CO2 and 13CO2 incubation fluxes from five Hawaiian soils. *Biogeochemistry*, *38*(1), 1–17.

Trumbore, S. (2009). Radiocarbon and Soil Carbon Dynamics. *Annual Review of Earth and Planetary Sciences*, *37*(1), 47–66.

von Lützow, M., Kögel-Knabner, I., Ekschmitt, K., Matzner, E., Guggenberger, G., Marschner, B., & Flessa, H. (2006). Stabilization of organic matter in temperate soils: Mechanisms and their relevance under different soil conditions - A review. *European Journal of Soil Science*, *57*(4), 426–445.

Wada, K. (1989). Allophane and Imogolite. In *Minerals in Soil Environments* (pp. 1051–1087). Soil Science Society of America.

Whalen, J. K., Bottomley, P. J., & Myrold, D. D. (2000). Carbon and nitrogen mineralization from light- and heavy-fraction additions to soil. *Soil Biology and Biochemistry*, *32*(10), 1345–1352.

Whitman, T., Zhu, Z., & Lehmann, J. (2014). Carbon mineralizability determines interactive

effects on mineralization of pyrogenic organic matter and soil organic carbon. *Environmental Science and Technology*, *48*(23), 13727–13734.

Xu, X., Zhou, Y., Ruan, H., Luo, Y., & Wang, J. (2010). Temperature sensitivity increases with soil organic carbon recalcitrance along an elevational gradient in the Wuyi Mountains, China. *Soil Biology and Biochemistry*, *42*(10), 1811–1815.

Zimmerman, A. R., Gao, B., & Ahn, M.-Y. (2011). Positive and negative carbon mineralization priming effects among a variety of biochar-amended soils. *Soil Biology and Biochemistry*, *43*(6), 1169–1179.

CH. 3: CONCLUSION

Summary of Findings

The results of this study demonstrate the dominant role played by proximal controls in predicting the potential decomposition of soil organic matter (SOM). Significant predictors of cumulative specific respiration (CSR), a metric of the decomposability of SOM, common to both horizons included non-crystalline minerals and SOM chemistry. Additionally, the proportion of organic C in the occluded fraction was a significant predictor for CSR in B horizons; however, this is likely an experimental artifact due to the potential accidental inclusion of fine roots in at least some of the incubation samples. In both A and B horizons, the fast-cycling pool decomposition rate (k_{fast}) was predicted by SOM chemistry, specifically the quantity of pyrogenic C present. Other k_{fast} controls in A horizons included several predictors related to the influence of the aboveground environment on A horizons, including sodium pyrophosphate extractable Mn, land cover, and mean annual precipitation. Controls of k_{fast} unique to B horizons included bulk soil %N and depth. There were no slow-cycling pool decomposition rate (k_{slow}) predictors common to both pools. Climate and non-crystalline minerals controlled k_{slow} in A horizons, while k_{slow} in B horizons was controlled by bulk soil C:N ratio and the proportion of organic C in the occluded fraction, which again is likely an experimental artifact.

Limitations, Implications, and Proposed Future Research

As mentioned in chapter 2, laboratory incubations, like all methods used to study soil C dynamics, have several drawbacks, including artificial temperature and moisture regimes, destruction of soil structure, and the exclusion of plant inputs (Torn et al., 2009). Given these issues and evidence for calculated decomposition rates being method dependent (Feng et al., 2016), decomposition rates calculated from laboratory incubations should generally not be extrapolated to a field setting (Torn et al., 2009). How should the results from this study be interpreted then? Although it may not be advisable to parameterize soil sub-models from Earth system models (ESMs) using our incubation data, the results from the incubation indicate what variables should potentially be incorporated into the next generation of ESM soil sub-models.

The inclusion of metrics of non-crystalline minerals as significant predictors of CSR in both horizons and k_{slow} in A horizons supports the emerging consensus of the need to move beyond clay as a simple proxy for SOM stabilization via mineral associations (Rasmussen et al., 2018). The primary justification for the use of clay as a proxy for mineral-controlled stabilization is percent clay data is widely available. Although this is certainly true, there is abundant evidence that the type of secondary minerals in the clay-size fraction is vital in SOM-mineral interactions, and as such, all clay-sized particles should not be viewed as having the same effect on SOM stabilization. Consequently, a proposed future research direction is to incorporate existing data sets related to the distribution of non-crystalline minerals, such as the USDA NRCS Soil Survey Geographic Database (SSURGO), into Earth system models.

For B horizons, an increase in nitrogen (N) availability had a significant positive effect on both k_{fast} and k_{slow}, which suggests that N is a limiting factor for decomposition in B horizons.

This is consistent with several other laboratory incubation studies that found an increase in decomposition rates with the addition of N to B horizon samples (Fierer et al., 2003; Tian et al., 2016). However, this seemingly contradicts a large body of literature that has found that decomposition rates decreased with increased N inputs (e.g., Cusack, Torn, Mcdowell, & Silver, 2010; Frey et al., 2014; Ramirez, Craine, & Fierer, 2012). What appears to be driving this difference is horizon as the studies cited above that found N additions to have a negative impact on decomposition rates used soils from only the top 10 cm of the soil profile. Consequently, it appears that the impact of altered N inputs on a given system will depend in part on how N inputs change throughout the soil profile. If N inputs increase in lower horizons, then it is possible that SOM decomposition will be enhanced, at least partly offsetting any decreases in decomposition in upper horizons. Regardless, the effect of N on decomposition strongly suggests that alterations to the N cycle must be included in the suite of global change drivers considered in future studies.

Lastly, the results of this study lead to a broader question regarding the controls on SOM decomposition. Since soil bacteria and fungi are the primary agents of SOM decomposition, do soil microbes need to be explicitly represented in models of SOM decomposition? Or is the reality that microbial community composition and dynamics are largely governed by soil physicochemical properties and other external factors, resulting in it being unnecessary to explicitly represent microbes in such models? Although the results of this study suggest the latter conclusion to some degree, there is still a relatively large amount of variance not explained in our regression analysis, especially for k_{slow}. It is possible that this variance is largely attributable to the characteristics of the soil microbial community. Furthermore, different types of models (statistical vs. processed-based) would have different requirements, with process-based models

likely requiring the inclusion of the soil microbial community to accurately represent SOM decomposition. Consequently, future SOM decomposition research should incorporate the soil microbial community and explore interactions between the microbial community and physicochemical environment.

References

Cusack, D. F., Torn, M. S., Mcdowell, W. H., & Silver, W. L. (2010). The response of heterotrophic activity and carbon cycling to nitrogen additions and warming in two tropical soils. *Global Change Biology*, *16*(9), 2555–2572.

Feng, W., Shi, Z., Jiang, J., Xia, J., Liang, J., Zhou, J., & Luo, Y. (2016). Methodological uncertainty in estimating carbon turnover times of soil fractions. *Soil Biology and Biochemistry*, *100*, 118–124.

Fierer, N., Allen, A. S., Schimel, J. P., & Holden, P. A. (2003). Controls on microbial CO 2 production: A comparison of surface and subsurface soil horizons. *Global Change Biology*, *9*(9), 1322–1332.

Frey, S. D., Ollinger, S., Nadelhoffer, K., Bowden, R., Brzostek, E., Burton, A., … Wickings, K. (2014). Chronic nitrogen additions suppress decomposition and sequester soil carbon in temperate forests. *Biogeochemistry*, *121*(2), 305–316.

Ramirez, K. S., Craine, J. M., & Fierer, N. (2012). Consistent effects of nitrogen amendments on soil microbial communities and processes across biomes. *Global Change Biology*, *18*(6), 1918–1927.

Rasmussen, C., Heckman, K., Wieder, W. R., Keiluweit, M., Lawrence, C. R., Berhe, A. A., …

Wagai, R. (2018). Beyond clay: towards an improved set of variables for predicting soil organic matter content. *Biogeochemistry*, *137*(3), 297–306.

Tian, Q., Yang, X., Wang, X., Liao, C., Li, Q., Wang, M., … Liu, F. (2016). Microbial community mediated response of organic carbon mineralization to labile carbon and nitrogen addition in topsoil and subsoil. *Biogeochemistry*, *128*(1–2), 125–139.

Torn, M. S., Swanston, C. W., Castanha, C., & Trumbore, S. E. (2009). Storage and Turnover of Organic Matter in Soil. In *Biophysico-Chemical Processes Involving Natural Nonliving Organic Matter in Environmental Systems* (pp. 219–272).

APPENDIX A: CORRELATION COEFFICIENTS AND P-VALUES

Table A1 Spearman's rank correlation coefficients (ρ) and corresponding P-values (in italics) from Fig. 2.2. Response variables are grouped by horizon (A and B), and cells with P-values > 0.05 have been shaded. Note that this table continues on the next page.

		Climate							**Soil Physical Properties**			**Soil Chemical Properties**									
		MAT	**MST**	**Inc. Temp.**	**MAP**	**PET**	**PET Ratio**	**MAP - PET**	**Depth**	**% clay**	**% sand**	**pH**	**Mag. Sus.**	**Ca (AA)**	**Mg (AA)**	**Ca + Mg (AA)**	**Na (AA)**	**Al (AA)**	**Al (KCl)**	**Al (AO)**	**Al (DC)**	**Al (SP)**
A	**CSR (0-52 weeks)**	0.210	0.316	0.244	-0.468	-0.568	0.595	-0.568	-0.134	-0.289	0.247	0.454	-0.332	0.153	-0.009	0.173	-0.239	-0.597	-0.441	-0.608	-0.536	-0.448
		0.375	*0.175*	*0.300*	*0.037*	*0.009*	*0.006*	*0.009*	*0.572*	*0.217*	*0.295*	*0.044*	*0.152*	*0.519*	*0.970*	*0.466*	*0.310*	*0.005*	*0.052*	*0.004*	*0.015*	*0.048*
	k (fast pool)	-0.125	-0.111	-0.034	0.266	0.283	-0.263	0.283	0.399	0.557	-0.608	0.041	0.175	0.165	0.310	0.177	0.062	0.102	-0.382	0.472	0.548	0.685
		0.600	*0.640*	*0.887*	*0.256*	*0.227*	*0.262*	*0.227*	*0.081*	*0.011*	*0.004*	*0.865*	*0.460*	*0.486*	*0.184*	*0.454*	*0.796*	*0.668*	*0.097*	*0.036*	*0.012*	*0.001*
	k (slow pool)	0.186	0.242	0.231	-0.127	-0.308	0.341	-0.308	0.124	-0.059	0.003	0.374	-0.175	0.215	0.164	0.223	-0.212	-0.535	-0.549	-0.392	-0.305	-0.129
		0.433	*0.304*	*0.328*	*0.593*	*0.186*	*0.141*	*0.186*	*0.603*	*0.806*	*0.990*	*0.104*	*0.460*	*0.363*	*0.490*	*0.346*	*0.369*	*0.015*	*0.012*	*0.087*	*0.190*	*0.587*
B	**CSR (0-52 weeks)**	0.193	0.313	0.314	-0.114	-0.182	0.205	-0.182	0.388	-0.060	0.158	0.045	-0.446	0.032	0.090	0.075	-0.232	-0.256	-0.221	-0.589	-0.418	-0.180
		0.414	*0.179*	*0.178*	*0.633*	*0.443*	*0.387*	*0.443*	*0.091*	*0.801*	*0.506*	*0.850*	*0.049*	*0.895*	*0.705*	*0.753*	*0.326*	*0.277*	*0.349*	*0.006*	*0.067*	*0.446*
	k (fast pool)	-0.296	-0.302	-0.308	-0.264	-0.197	0.221	-0.197	0.416	0.375	-0.532	0.406	0.453	0.358	0.398	0.364	0.519	-0.362	-0.461	0.174	0.152	0.132
		0.206	*0.195*	*0.187*	*0.260*	*0.405*	*0.349*	*0.405*	*0.068*	*0.103*	*0.016*	*0.076*	*0.045*	*0.121*	*0.082*	*0.115*	*0.019*	*0.116*	*0.041*	*0.462*	*0.523*	*0.578*
	k (slow pool)	0.066	0.140	0.103	-0.153	-0.017	0.054	-0.017	0.379	0.061	-0.003	0.126	-0.277	0.188	0.192	0.214	-0.027	-0.194	-0.213	-0.183	-0.020	-0.113
		0.782	*0.556*	*0.665*	*0.520*	*0.945*	*0.821*	*0.945*	*0.099*	*0.799*	*0.990*	*0.596*	*0.237*	*0.427*	*0.416*	*0.366*	*0.910*	*0.413*	*0.367*	*0.439*	*0.935*	*0.636*

		Soil Chemical Properties										SOM Properties						Distribution of SOM				Py-C Properties		
		Fe (KCl)	Fe (AO)	Fe (DC)	Fe (SP)	Mn (AO)	Mn (DC)	Mn (SP)	Si (AO)	Si (DC)	Si (SP)	FLF %C	OCC %C	HF %C	Bulk soil %N	Bulk soil C:N ratio	Bulk soil d13C	Prop. C in FLF	Prop. C in OCC	Prop. C in FLF + OCC	Prop. C in HF	BPCA total/ soil	BPCA total/ total org. C	B6CA/ BPCA total
A	**CSR (0-52 weeks)**	-0.178	-0.645	-0.430	-0.574	-0.417	-0.289	-0.281	-0.421	-0.151	-0.229	-0.152	-0.420	-0.559	-0.454	-0.507	0.045	0.116	0.032	0.099	-0.099	-0.658	-0.389	-0.316
		0.452	*0.002*	*0.058*	*0.008*	*0.068*	*0.217*	*0.230*	*0.065*	*0.526*	*0.332*	*0.522*	*0.066*	*0.010*	*0.044*	*0.023*	*0.850*	*0.627*	*0.895*	*0.677*	*0.677*	*0.002*	*0.090*	*0.174*
	k (fast pool)	-0.325	0.370	0.377	0.645	0.537	0.546	0.615	0.369	0.378	0.583	-0.355	0.027	0.581	0.421	-0.373	0.093	-0.621	-0.377	-0.623	0.623	0.114	0.017	0.233
		0.162	*0.108*	*0.101*	*0.002*	*0.015*	*0.013*	*0.004*	*0.109*	*0.100*	*0.007*	*0.124*	*0.910*	*0.007*	*0.064*	*0.105*	*0.696*	*0.003*	*0.101*	*0.003*	*0.003*	*0.633*	*0.945*	*0.324*
	k (slow pool)	-0.386	-0.477	-0.254	-0.296	-0.211	-0.090	-0.055	-0.124	0.041	0.005	-0.125	-0.205	-0.284	-0.167	-0.457	0.232	0.123	-0.006	0.107	-0.107	-0.394	-0.132	-0.056
		0.093	*0.034*	*0.280*	*0.205*	*0.373*	*0.705*	*0.818*	*0.603*	*0.865*	*0.985*	*0.600*	*0.387*	*0.225*	*0.482*	*0.043*	*0.326*	*0.605*	*0.980*	*0.654*	*0.654*	*0.085*	*0.578*	*0.813*
B	**CSR (0-52 weeks)**	0.014	-0.511	-0.277	-0.236	-0.254	-0.264	-0.318	-0.518	-0.117	-0.063	0.150	-0.004	-0.558	-0.592	-0.332	-0.128	0.305	0.466	0.430	-0.430	-0.440	-0.104	-0.142
		0.952	*0.021*	*0.238*	*0.316*	*0.280*	*0.260*	*0.171*	*0.019*	*0.624*	*0.791*	*0.527*	*0.987*	*0.011*	*0.006*	*0.152*	*0.591*	*0.191*	*0.038*	*0.058*	*0.058*	*0.052*	*0.663*	*0.552*
	k (fast pool)	-0.532	0.265	0.232	0.183	0.469	0.512	0.420	0.485	0.359	0.295	-0.072	0.042	0.304	0.320	-0.218	0.334	-0.468	-0.051	-0.317	0.317	-0.135	-0.400	-0.333
		0.016	*0.259*	*0.326*	*0.439*	*0.037*	*0.021*	*0.065*	*0.030*	*0.120*	*0.207*	*0.762*	*0.860*	*0.192*	*0.169*	*0.356*	*0.150*	*0.038*	*0.830*	*0.173*	*0.173*	*0.570*	*0.081*	*0.152*
	k (slow pool)	-0.113	-0.274	-0.009	-0.189	-0.029	0.032	-0.265	-0.075	0.207	0.015	-0.226	0.087	-0.179	-0.098	-0.520	0.023	0.104	0.176	0.173	-0.173	-0.409	-0.320	-0.265
		0.635	*0.243*	*0.970*	*0.424*	*0.905*	*0.892*	*0.258*	*0.755*	*0.382*	*0.950*	*0.339*	*0.715*	*0.451*	*0.682*	*0.019*	*0.925*	*0.663*	*0.458*	*0.466*	*0.466*	*0.073*	*0.169*	*0.259*

Py-C, pyrogenic C; CSR, cumulative specific respiration; MAT, mean annual temperature; MST, mean summer temperature; Inc. Temp., incubation temperature; MAP, mean annual precipitation; PET, potential evapotranspiration; Potential ET Ratio = PET/MAP; Mag. Sus., magnetic susceptibility; AA, ammonium acetate extractable; AO, ammonium oxalate extractable; DC, dithionite-citrate extractable; SP, sodium pyrophosphate extractable; FLF, free light fraction; OCC, occluded fraction; HF, heavy fraction; BPCA, benzenepolycarboxlyic acids